

Short running page heading: **Rib cage mechanics in aquatic mammals**

Title: **Farewell to life on land—thoracic strength as a new indicator to determine paleoecology in secondary aquatic mammals**

Authors: **Konami Ando¹ and Shin-ichi Fujiwara²**

Affiliations: ¹Department of Earth and Planetary Sciences, Graduate School of Environmental Studies, Nagoya University, Furocho, Chikusa, Nagoya, Aichi, 464-8601, Japan

²The Nagoya University Museum, Furocho, Chikusa, Nagoya, Aichi, 464-8601, Japan

Summary: Habitat shifts from land to water have occurred independently in several mammal lineages. However, because we do not know completely about the relationship between skeletal morphology and function, both reliable life reconstructions of each extinct taxon and the timing of those shifts in locomotor strategies are yet to be fully understood. We estimated the strengths of rib cages against vertical compression in 26 extant and 4 extinct mammal specimens including cetartiodactyls, paenungulates, and carnivorans, representing 11 terrestrial, 6 semi-aquatic, and 9 obligate aquatic taxa. Our analyses of extant taxa showed that strengths were high among terrestrial/semi-aquatic mammals, whose rib cages are subjected to vertical compression during the support on land, whereas strengths were low among obligate aquatic mammals, whose rib cages are not subjected to antigravity force in the water. We therefore propose rib strength as a new index to estimate the ability of an animal to be supported on land while being supported by either the forelimbs or thoracic region. According to our analyses of extinct taxa, this ability to be supported on land was rejected for a basal cetacean (Cetartiodactyla: *Ambulocetus*) and two desmostylians (Paenungulata: *Paleoparadoxia* and *Neoparadoxia*). However, this ability was not rejected for one desmostylian species (*Desmostylus*). Further study of the ribs of extant/extinct semi-aquatic taxa may help in understanding the ecological shifts in these groups.

Keywords: rib, desmostylian, early cetacean, reconstruction, aquatic

Introduction

Tetrapoda is a group of vertebrates which shifted their ecospace from water to land in the Late Devonian (Ahlberg, 1995; Pierce et al., 2012), and later became quite diversified in their lifestyles. Many tetrapod taxa have secondarily shifted their habitat from land to water. Among mammals (Tetrapoda), whales and sirenians are known to have evolved from terrestrial-quadrupedal origins and have acquired obligate aquatic lifestyles independently (Nishihara et al., 2005; Wang and Yang, 2013). The evolutionary process of the shifts in ecospace in these lineages and its relationship with paleoenvironmental changes has occupied the attention of researchers in the fields of paleoecology and paleoenvironmentology (e.g., Lipps and Mitchell, 1976; Suto et al. 2012; Pyenson et al., 2014).

According to the fossil record, obligate aquatic mammals are thought to have gradually shifted from a terrestrial to semi-aquatic to obligate-aquatic lifestyle (Gingerich, 2003), by involving extension of the lumbar area, transitions from limbs to fins, and degeneration of hindlimbs (Howell, 1930; Gingerich, 2003). Taxa in the early stages of these shifts that retained all four limbs have been reconstructed as amphibious animals, due to the presence of four limbs, as well as the geological settings of the fossil deposits, and the stable isotope analyses of the teeth (e.g., Desmostylia: *Desmostylus* and *Paleoparadoxia*; Sirenia: *Pezosiren*; Cetacea: *Pakicetus* and *Ambulocetus*: Thewissen, Hussain, and Arif, 1994; Yamazaki and Ikeuchi, 2000; Thewissen et al., 2001; Domning, 2001; Domning, 2002; Inuzuka, 2005).

But, how can we tell reliably whether these animals retained the ability to walk on land? Relationships between their skeletal morphologies and these functions have rarely been confirmed by biomechanical studies. It is therefore difficult to reliably reconstruct lifestyles from the skeletal morphologies in these extinct taxa. It is also hard to determine when or in which stage of evolution the habitats of these taxa shifted. Specifically, in which stages they shifted to the obligate aquatic lifestyle remains unclear.

In arguments concerning habitat shifts from terrestrial to obligate aquatic lifestyles in secondarily aquatic taxa, we should take into account not only acquiring the ability to swim but also loss of the ability of terrestrial locomotion. Otherwise, we cannot determine whether the extinct taxa, especially the ones with limbs, such as desmostylians and early cetaceans, were obligate aquatic mammals (which spend their whole life in water) or semi-aquatic taxa (which occasionally move on land). We therefore focused our attention on the use of an indicator for non-terrestriality for more reliable life-reconstructions in extinct taxa.

The aim of this study is to propose a quantitative biomechanical index to determine the presence or absence of terrestriality. This study also aims to reconstruct the paleoecology of some extinct taxa.

We focused on the strength of the rib cage as an indicator of terrestriality. In quadrupedal postures, serratus muscles which originate from the lateral sides of thoracic ribs and insert onto the dorsal margin of the scapula, function to lift up the rib cage during the stance phase (Fujiwara et al., 2009). The thoracic ribs are subjected to a vertical compression between the downward body weight and the upward lifting force (Fig. 1A). Thoracic ribs in both terrestrial and semi-aquatic quadrupeds are subjected to vertical compression on

land. A rib cage in crawling posture, like seals on land being supported by their sterna, is also subjected to vertical compression between the downward body weight and the upward lifting force on the distal ends of the thoracic ribs (Fig. 1B). On the other hand, obligate aquatic taxa do not support their bodies by their forelimbs or by their sterna. In other words, thoracic ribs in obligate aquatic mammals are not necessarily adapted for sustaining vertical/uni-directional compression (Fig. 1C). From the above, we hypothesized that the thoracic strengths in obligate aquatic mammals are de-emphasized in relation to their body size compared with those in terrestrial/semi-aquatic quadrupeds.

Materials and Methods

Materials

Thoracic skeletons (ribs and vertebrae) of 26 extant mammalian taxa (17 cetartiodactyls, 4 paenungulates, and 5 carnivorans) were used to test the abovementioned hypothesis (Table 1). Cetartiodactyls and paenungulates are monophyletic groups which include both extant terrestrial/semi-aquatic quadrupeds and extant obligate aquatic taxa, and are therefore the best taxa to test differences in thoracic strengths within the group. Aquatic lifestyles in cetaceans (Cetartiodactyla) and sirenians (Paenungulata) were derived from terrestrial quadrupedal ancestors (Fig. 2: Nishihara et al., 2005; Wang and Yang, 2013). There are no obligate aquatic carnivorans, but the group includes some extant semi-aquatic taxa that are highly adapted for swimming, such as pinnipeds and lutrines. The carnivorans are selected, therefore, to test the difference in thoracic strengths between terrestrial and semi-aquatic taxa.

We also used 4 extinct taxa, including 1 early cetacean (Cetartiodactyla) and 3 desmostylians (Paenungulata) to estimate their paleoecologies (Table 1). We chose extinct taxa that are phylogenetically bracketed within the extant study taxa (Fig. 2: Witmer, 1995), and which retained their limbs to test whether these animals retained the ability to move on land. We selected fossil specimens whose bone deformations after burial were expected to be minimal, and whose thoracic skeletons were nearly completely preserved (Tokunaga, 1939; Shikama, 1966; Thewissen et al., 1994; Inuzuka, 2005; Domning and Barnes, 2007).

Body mass data were not recorded for most extant specimens. For those specimens, the body masses were inferred from the literature. For *Oryx*, *Giraffa*, and *Kogia* specimens, which were determined to be young or sub-adult due to incomplete ossification in their centra, we used the lowest body mass (Table 1: Stewart, 1963; Nowak, 1999). For the *Lagenorhynchus* specimen, the largest class (in terms of body mass) of the taxa, we used the largest body mass data in the literature (Table 1: Nowak, 1999). The *Elephas* specimen was female (Table 1). Therefore, the average body mass data for female *Elephas* was used (Nowak, 1999). In the other extant specimens with no body mass data, the averages of the largest and smallest body mass data were used (Table 1). Body masses of extinct specimens were estimated (Table 1: Thewissen et al., 1994; Inuzuka, 1996, 2005).

Mechanical Model

It is assumed that a vertebra and a pair of associated ribs are firmly connected to each other to form an arch in dorsal-side-up position (Fig. 3). The mechanical stresses on thoracic ribs during the stance phase in quadrupeds (Fig. 1A,B) are assumed such that the centrum on the vertebra is fixed to avoid three-dimensional translations and rotations, and the static vertical upward lifting force P [N] is applied to the distal end of each rib (Fig. 3A). In order to simplify the model, we also assumed that rib pairs are symmetric with each other in shape and are articulated symmetrically to the vertebra. The arch is vertically compressed between the upward lifting force on the distal ends of right and left ribs ($2P$ [N] in total) and the downward force ($-2P$ [N]) caused by the body weight on the centrum (Fig. 1A). Due to the rib curvatures, bending stresses are distributed in the rib under vertical compression—compressive and tensile stresses, respectively, are distributed in the medial and lateral sides of the rib. In this situation, the bending stresses are defined as positive, and absolute values of minimum compressive and maximum tensile stresses produced in the transverse section of the rib are equal. Therefore, the maximum bending stress σ_m [MPa] at a certain section of the rib is defined as follows:

$$\sigma_m = M/Z$$

where M [Nmm] is the bending moment at the section, and Z [mm³] is the section modulus. The bending moment M [Nmm] is formulated as follows:

$$M = P \times L$$

where L [mm] is the bending moment arm that is the distance from the section to the vector of the vertical force P [N] (Fig. 3A). The section modulus Z [mm³] is an index of the difficulty of bending the beam structure which is specific to the cross-sectional shape. In order to simplify the model, we assumed that the cross-section of the rib is oval, and Z is calculated by the following equation:

$$Z = \frac{\pi w^2 t}{4}$$

where w [mm] is half of the cranio-caudal width of the transverse section, and t [mm] is half of the inferior-superior thickness of the section (Fig. 3A).

If σ_m reaches the yield stress [MPa], the rib is fractured at the section. The yield stress is specific to the material. The tensile strength (yield stress, 200 MPa) and the compressive strength (yield stress, -170 MPa) of cortical bones in large mammals were assigned for the estimation in this study (Vogel, 2003). The validity of assigning material properties to cortical bone for all the study specimens will be discussed later. The bones of mammals are weak against compression compared to tension. Therefore, we assumed that the rib fractures if σ_m reaches 170 MPa (absolute value of compressive strength). The minimum force P_m [N] that causes fractures at a certain point on a single side of the rib is estimated as follows:

$$P_m = \frac{\sigma_m Z}{L} = \frac{170\pi w^2 t}{4L}$$

The bending moment arm (L), the width ($2w$) and the thickness ($2t$) of the rib section are available from the measurements on the specimens (Fig. 3B).

On the assumption that the left and right ribs are symmetric in shape, we defined the sum of P_m s on left and right ribs ($2P_m$) as the fracture load (F_m) that causes fractures at certain points on the ribs (Fig. 3). According to Fujiwara et al. (2009), the maximum stress on the rib is located at the neck or at the lateral-most point on the curvature of the rib (Fig. 3A). We therefore estimated fracture load on the neck (F_n [N]) and on the lateral-most (F_l [N]) points on the curvature of the rib shaft of each rib for the two different points (at the neck and the lateral-most point on the curvature) (Fig. 3; Table S1). The more complete rib of each pair in terms of preservation was chosen for the measurements. The fracture load that was the smaller of the loads at these two points is defined as the fracture load (F [N]) of the arch ($F = F_n$ when $F_n < F_l$; $F = F_l$ when $F_n > F_l$; Fig. 3). We also standardized F by body weight (N). The body weights, with gravitational acceleration (9.8065 m/s^2), were calculated from the body mass data (Table 1).

With terrestrial support on the forelimbs or sterna (Fig. 1A, B), it is expected that the vertical reaction force on the sternum is mostly transmitted to the distal-most points on the true ribs that have direct skeletal connections to the sternum. We therefore defined the sum of fracture loads of the true ribs (TF [N]) as the thoracic strength of the specimen (e.g., thoracic strength [TF] in *Bos* is a sum of F s from the first to sixth ribs [the true ribs]; Table S1). The calculations and drawing of the graphic chart were conducted by using R 3.2.2 (R Foundation for Statistical Computing).

Measurements

The moment arm of the fracture load (L), the width ($2w$), and the thickness ($2t$) of the transverse section of the rib are required to estimate the fracture load (F). Of these, measurements of the width ($2w$) and the thickness ($2t$) were taken directly on the skeletons of the study specimens by using a vernier caliper (0–200 mm; accuracy, 0.01 mm; CD-20CPX, Mitutoyo Co., Ltd.).

We could not measure directly the moment arms of the fracture loads (L_m) on the study specimens because no landmarks could be used to measure the foot of the moment arm on the skeleton (Fig. 3A). Therefore, the medio-lateral distances of the neck (L_n) and the lateral-most point on the rib curvature (L_l) from the upward vector P (Fig. 3A) were measured in three different ways depending on the specimens:

(1) With mounted specimens, the measurements were taken directly on the skeletons using the abovementioned vernier caliper or a Martin-type anthropometer (200–2000 mm; accuracy, 1 mm). Measurements were taken for widths between the distal ends ($2d$), the necks ($2n$), and the lateral-most points ($2l$) of the left and right ribs (Fig. 3B). The moment arms L_n and L_l were defined, respectively, as $|d - n|$ and $|d - l|$.

(2) With relatively small unmounted specimens, a set of vertebra and ribs were firmly connected to each other at the articular surfaces of the costovertebral joint before measurements. The arch of the ribs and

vertebra together was photographed from the caudal side with graph paper ruled into 1 mm squares as the background. These photographs were taken from as far as possible to minimize the influence of skewness of the lens and parallax. The photographs were then scaled based on grid size. The orientation of the neural spine on the photograph was defined as the dorso-ventral axis, and the line perpendicular to the axis was defined as the medio-lateral axis. L_n and L_l were determined to be differences between medio-lateral components from the distal end to the neck and to the lateral-most point of the rib, respectively.

(3) With relatively large unmounted specimens, the vertebra and ribs were laser-scanned using Kinect (Microsoft Co.), and the three-dimensional (3-D) polygons of the skeletons were constructed on a computer using 3-D data editing software (Artec Studio 9, Datadesign Co., Ltd.). The 3-D skeletal models were set dorsal-side-up, and the measurements L_n and L_l were taken on the 3-D model— L_n and L_l were determined to be differences between horizontal components from the distal end to the neck and to the lateral-most point of the rib, respectively. The resolution of the scanner (2 mm when laser-scanned at 1 m distance: Khoshelham and Elberink, 2012) is considered to be negligible in relation to the scale of the specimens (*Berardius* and *Elephas*; Tables 1, S1).

Results

Fracture loads on each rib in the study specimens are listed in Table S1. Both terrestrial and semi-aquatic quadrupeds emphasized the estimated fracture loads (F) in true ribs, in contrast to the F values in false and floating ribs (Table S1). F values in the first ribs were especially emphasized in *Bos*, *Oreamnos*, *Tragelaphus*, and *Lama glama* (Table S1). In *Elephas*, F values in the first three ribs were pronounced—the fracture load standardized by the body weight (safety factor) exceeded 2.00 in these ribs (Table S1). In these terrestrial and semi-aquatic taxa, the ratios of thoracic strength (TF [N]) to the total of F values in the specimen (RF [N]: sum of F values in all ribs, including true, false, and floating ribs) exceed around 0.88–0.89% on average (Table 1). There was little difference in the ratio (TF/RF [N/N]) between terrestrial and semi-aquatic taxa—both of which can be supported on land by lying on their thorax (Table 1). The high TF/RF values in these taxa suggest that the contribution of the true ribs to strength against vertical compressions is relatively high.

On the other hand, the F values were not emphasized in any ribs among true, false, and floating ribs in obligate aquatic taxa (cetaceans and sirenians: Table S1). The ratios (TF/RF) were relatively low (0.66 on average) in these taxa (Table 1).

Relationships between body mass and thoracic strength (N) in the study specimens are shown in Fig. 4. Body mass was positively-correlated with thoracic strengths in terrestrial quadrupeds, semi-aquatic quadrupeds, and obligate aquatics (Fig. 4). Correlation coefficients of the regression lines were high ($R=0.999$ in terrestrial quadrupeds; $R=0.867$ in semi-aquatics) in terrestrial and semi-aquatic quadrupeds, but were relatively low in obligate aquatic mammals ($R=0.690$).

The regression lines for the terrestrial and semi-aquatic quadrupeds were similar to each other, although the intercept of the line was slightly larger in semi-aquatics than in terrestrials. Both terrestrial and semi-aquatic carnivoran taxa showed relatively high thoracic strengths for their body mass compared to those in terrestrial and semi-aquatic cetartiodactyls and paenungulates (Fig. 4). The intercept of the regression line was small in obligate aquatic taxa.

Relationships between body masses and thoracic strengths standardized by body weight are shown in Fig. 4. In all terrestrial and semi-aquatic taxa, thoracic strengths were no less than $7.35 \times$ body weight (N). Among the terrestrial and semi-aquatic taxa, thoracic strengths per body weight in carnivorans tend to be higher than those in the cetartiodactyls and paeungulates (Fig. 4).

Thoracic strengths in obligate aquatic taxa tended to be lower than those in terrestrial and semi-aquatic taxa, but the value varied by taxon (Fig. 4). Thoracic strengths were $0.32 \sim 4.92 \times$ body weight in most cetaceans and *Trichechus* (sirenians). However, the value was higher in the *Dugong* specimen (sirenians), whose value was comparable to those in terrestrial and semi-aquatic taxa ($7.58 \times$ body weight: Fig. 4).

Thoracic strengths estimated in extinct taxa are shown in Fig. 4, and Table S1. In *Ambulocetus* (early cetacean), *Paleoparadoxia*, and *Neoparadoxia* (desmostylians), the fracture loads (F) for each rib were especially low ($2.37 \sim 3.59 \times$ body weight: Table S1). Thoracic strengths in these three taxa were similar to those in extant obligate aquatics (Fig. 4). The thoracic strength in *Desmostylus* (desmostylians), however, was as high as those in terrestrial/semi-aquatic quadrupeds ($7.40 \times$ body weight: Fig. 4).

Discussion

The strength analyses of the rib cages of extant mammals reveal that thoracic strengths in terrestrial and semi-aquatic quadrupeds exceed a certain level ($> 7.35 \times$ body weight). During terrestrial locomotion in mammals, the limb skeletons usually bear the peak stresses, which range from one quarter to one half of the fracture loads (Biewener, 1990). The relatively high rib strengths for the body masses estimated in quadrupeds are consistent with the idea that the thoracic ribs in quadrupeds are subjected to vertical compression during locomotion (Fujiwara et al., 2009). High correlation coefficients of the regression lines in terrestrial ($R=0.999$) and semi-aquatic quadrupeds ($R=0.867$) indicate that thoracic strength is strongly related to the function of the body support. The differences in thoracic strengths between terrestrial/semi-aquatic carnivorans and terrestrial/semi-aquatic cetartiodactyls and paenungulates may reflect differences of the lineages (Figs. 2 and 4).

On the other hand, the rib cages in obligate aquatics are not subjected to vertical compression in the water; therefore, their rib cages have no need for retaining their strength against vertical compression. Compared with those of quadrupeds, de-emphasized thoracic strengths in most obligate aquatic mammals (Fig. 4) are consistent with this idea. In theory, the taxa whose ratio of thoracic strength to body weight exceeds more than 1.00 may be able to support their bodies on land while resting on either forelimbs or

thoraxes. Relatively low correlation coefficient in obligate aquatic mammals ($R=0.690$) suggests that thoracic strength and body mass are less relevant in these animals. The relatively small cetaceans, such as dolphins, can land on their bellies indeed. However, the strengths of rib cages for their body masses were much below the level of the terrestrial quadrupeds, and therefore they were not adapted for active quadrupedal motions or creeping-on-bellies on land. The thorax may be strengthened against vertical compression as well in obligate aquatic taxa, and some extant taxa, such as *Dugong* (Table 1), showed relatively high thoracic strength which was comparable to those in terrestrial taxa (Fig. 4). The thoracic strength in *Dugong* may be correlated with the ability of the terrestrial support on the belly or with any other biomechanical requirements on the thoracic bones which are yet to be known. The other strength analyses by assuming different mechanical conditions on the thorax, such as the resistance against hydrostatic pressure, may solve this problem.

From the above-mentioned points, thoracic strengths could become a reliable index to determine whether an animal had the ability to move on land, especially in extinct cetartiodactyls and paenungulates. Use of the strengths of rib cages was first introduced by Fujiwara et al. (2009) for estimating scapular position in terrestrial quadrupeds, but the strengths were estimated by using commercial software (Marc/Mentat, MSC Software Co., Ltd.: Fujiwara et al., 2009). We succeeded in improving the method in Fujiwara et al. (2009) by taking the thicknesses of ribs into account, as well as simplifying the measurement process, and using commonly used software (e.g., R; R Foundation for Statistical Computing).

Rib strengths in some extinct taxa that retained all four limbs were plotted within the distributions of extant obligate aquatic taxa ($\sim 3.59 \times$ body weight: Fig. 4). According to our analyses, *Ambulocetus*, *Paleoparadoxia*, and *Neoparadoxia* were determined to be non-terrestrial (obligate aquatic mammals) due to the absence of the thoracic strengths required for terrestrial support—thoracic strength would be a restricting factor for their terrestrial locomotion, though they do have limbs. The interpretation of *Paleoparadoxia* is consistent with the results of Hayashi et al. (2013) who reconstructed this animal as a shallow-water swimmer based on observations of its bone histology. On the other hand, our analysis did not reject the possibility of terrestrial locomotion in *Desmostylus*, which showed relatively high thoracic strength (Fig. 4).

Some other studies have offered interpretations different from our result, namely that *Ambulocetus* and desmostylians were capable of terrestrial locomotion on all four limbs or on bellies like extant seals (i.e., Thewissen and Hussain, 1994; Madar et al., 2002; Inuzuka, 2005; Inuzuka, 2009). These reconstructions were derived from the following skeletal features of their limbs and vertebrae which were similar in shape to extant semi-aquatic mammalian taxa – *Ambulocetus*: relatively robust forelimbs, short femur with relatively small area of the anti-gravity muscle attachments, shape of the vertebral column which is suitable for dorsoventral undulation (Thewissen and Hussain, 1994), robust sacrum which retains a firm connection to the ilium, and the vertebrae similar in shape to those of extant lutrines (Carnivora) (Madar et al., 2002); desmostylians: robust limb skeletons with relatively broad muscle attachments for pectoralis on the humerus

and sternum (Inuzuka, 1984). In order to make more reliable reconstructions of the extinct taxa, it is important to take the above-mentioned interpretations from the skeletal morphologies into account, in addition to our new index based on the thoracic strengths. But it is yet to be fully understood whether the strength of bone (e.g., Alexander, 1985; Biewener, 1990; Christian and Preuschoft, 1996) or the mechanical advantages of the musculoskeletal system (e.g., Fujiwara, 2009; Fujiwara and Hutchinson, 2012) in the axial and appendicular skeletons of these extinct taxa were sufficient for body support on land. An index for estimating animal ecology related to mechanical function becomes more powerful if the relationship between the index and animal ecology is shown to be consistent with the biomechanics and is also established in various species of extant taxa. Thoracic strength was proposed as one among many of those biomechanical indices to discriminate between terrestrial and obligate aquatic lifestyles in mammals. If additional biomechanical indices for estimating the capability of terrestrial locomotion from the limb or vertebral morphologies were proposed, and those indices were used together with thoracic strength, we expect that we could get much closer to a correct answer about the paleoecology of an extinct animal. Among the various stages of evolution from terrestrial to obligate aquatic taxa in the lineages of cetaceans and desmostylians, we only studied a limited number of the species (Table 1). To understand the ecological shifts along these lineages, it is worth estimating the thoracic strengths in the more basal and the more derived states within the studied taxa (e.g., Cetacea: *Rodhocetus*, *Pakicetus*, and *Dorudon*; Desmostylia: *Behemotops* and *Ashoroa*; Sirenia: *Pezosiren* and *Protosiren*: Inuzuka, 2005; Beatty, 2009; Domning, 2001; Thewissen et al., 2001), which is expected to be a challenging topic for future study.

There are some limitations of our study. The first limitation we discuss here is about the uncertainty of material properties in each bone of the study specimens. In order to simplify the model, we assigned material properties to cortical bone (Vogel, 2003) by assuming that all the skeletal materials used in this study were uniform and had no marrow cavities, when in fact, the bone densities vary with taxa, element, and also growth stage. The rib shafts in terrestrial taxa consist of cortical bones but are hollowed at the marrow cavity (Thewissen et al., 2009), whereas those in sirenians, *Ambulocetus*, and *Paleoparadoxia* consist of dense osteosclerotic cortical bone (Gray et al., 2007; Housaye, 2009; Buffrénil et al., 2010; Hayashi et al., 2013), and those in later-diverging cetaceans and *Desmostylus* consist of cancellous bone whose density is relatively low (Gray et al., 2007; Hayashi et al., 2013). These differences in bone density among the taxa may influence the yield stresses of the material as well as estimations of the thoracic strengths.

Even if the material properties of the inner layers of the bone varied among the study specimens, the peak stresses on the rib shafts are distributed at the external surface under vertical compression (Fujiwara et al., 2009). Therefore, our estimates of thoracic strength are likely appropriate in terrestrial/semi-aquatic extant taxa, sirenians, and paleoparadoxiids, the external layers of whose ribs consist of similar material—cortical bone.

On the other hand, yield stress in cancellous bone, which is relatively low in density, is smaller than that in cortical bone, which is relatively high in density (e.g., Keaveny et al., 2003; Bayraktar et al., 2004). If the difference in these yield stresses between cancellous and cortical bones were taken into account, the thoracic strengths in cetaceans and *Desmostylus* would be expected to be much lower than the strength estimated in this study (Table S1, Fig. 4). If so, the weaknesses of the thoracic strengths in cetaceans would be expected to be emphasized, and the thoracic strength of *Desmostylus* would be expected to deviate from the range of the strengths in extant terrestrial/semi-aquatic taxa.

The second limitation discussed here is the uncertainty of the body mass data and the center of mass position (Table 1). Most of the body mass data used in this study were not taken from the specimens when they were alive, but from the literature, due to the absence of specimen records. In terrestrial support, the thoracic ribs bear weight on the forelimbs, but do not sustain entire mass of the body. Therefore, the contributions to body support among forelimb, hindlimb, and abdomen for each studied taxa should also be concerned. Using the body mass data and the center of mass position of living specimens would provide more accurate estimations for our analyses of thoracic strengths.

The third limitation concerns the definition of the thoracic strengths. As mentioned above in the materials and methods section, thoracic strength was defined as the sum of vertical fracture loads on true ribs of the specimen. This is based on the assumption that the ground reaction force during a stance is mainly applied to the true ribs via serratus and pectoral muscles (Fujiwara et al., 2009), but the serratus muscles originate not only from true ribs but also may originate from the other ribs, such as false ribs (e.g., Nickel et al., 1986; Fujiwara et al., 2009). We did not take the strengths (fracture loads) of these false ribs into account, not only because it was difficult to determine which false ribs have the origins of serratus muscles from the skeletal specimens, but also because the serratus which originate from the false ribs tend to be more obliquely oriented and are expected to bear relatively little weight compared to the more vertically oriented serratus which originate from the true ribs. If further myological studies were carried out for these study taxa and their ribs were differentiated into two different types (the ribs with and without the origins of the serratus muscles), more precise estimation of the rib cage strength would be achieved from the method in this study. However, the fracture loads in the false ribs were relatively small (Table S1). Therefore, the estimations of thoracic strengths would not be changed dramatically, whether the false ribs were included or not in the estimation of the thoracic strength (TF [N]: Fig. 4).

Despite the above-mentioned limitations, this study reveals differences in thoracic strengths between the terrestrial/semi-aquatic quadrupeds and the obligate aquatic taxa. We expect that this new index proposed in this study can be used for clarifying when or in which stage of evolution some mammalian or other tetrapod lineages escaped from the land and shifted their habitats to the water.

Conclusion

A new method was proposed to estimate thoracic strength against dorso-ventral compression. A measure of this strength in 11 terrestrial, 6 semi-aquatic, and 9 obligate aquatic taxa representing three mammalian groups, two of which include taxa that have shifted from terrestrial quadrupeds to obligate aquatics, was analyzed in this study. The results show that the costal strengths relative to the body masses in obligate aquatic taxa are weaker than those in terrestrial and semi-aquatic quadrupeds. The index of costal strength can also be used as a quantitative tool to reconstruct locomotor behaviors in extinct taxa. Based on our new index, a basal cetacean (*Ambulocetus*) and two desmostylians (*Paleoparadoxia* and *Neoparadoxia*) were reconstructed as obligate aquatic mammals; however, terrestriality in another desmostylian (*Desmostylus*) was not rejected. Further analyses in other taxa may help in understanding the timings and evolution of secondary ecological shifts in the lineages of aquatic mammals.

Acknowledgments

This study was supported by a Japan Society for the Promotion of Science Fellowship (grant no. 25870305). The authors thank H. Hirotsu, H. Taru, R. Matsumoto (Kanagawa Prefectural Museum of Natural History, Odawara), T. Mochizuki (Iwate Prefectural Museum, Morioka), S. Kawabe (Gifu Prefectural Museum, Seki), S. Kawada, N. Kohno, T. Yamada, Y. Tajima (National Museum of Nature and Science, Tsukuba), M. Kurita, Y. Akune, H. Nitto (Nagoyako Aquarium, Nagoya), and M. Niimi (Nagoya University Museum, Nagoya) for giving us the chance to observe great specimens; and members of the Laboratory of Geobiology (Nagoya University) for many advices and comments. We thank two anonymous referees and the editor for improving this paper.

Author contributions

KA modified the methodology, conducted the experiments and analysis. SiF designed the study. Both KA and SiF wrote the manuscript. Both authors have no conflict of interest to declare.

Reference

- Ahlberg PE** (1995) *Elginerpeton pancheni* and the earliest tetrapod clade. *Nature* **373**, 420–425.
- Alexander R** (1985) *The Structure of Biological Science*. Cambridge: Cambridge University Press.
- Bayraktar HH, Morgan EF, Niebur GL, et al.** (2004) Comparison of the elastic and yield properties of human femoral trabecular and cortical bone tissue. *J Biomech* **37**, 27–35.
- Beatty BL** (2009) New material of *Cornwallius sookensis* (Mammalia: Desmostylia) from the Yaquina Formation of Oregon. *J Vert Paleont* **29**, 894–909.
- Biewener AA** (1990) Biomechanics of mammalian terrestrial locomotion. *Science* **250**, 1097–1103.
- Buffr nil V, Canoville A, D’Anastasio R, et al.** (2010) Evolution of sirenian pachyosteosclerosis, a model-case for the study of bone structure in aquatic tetrapods. *J Mamm Evol* **17**, 101–120.

- Christian A, Preuschoft H** (1996) Deducing the body posture of extinct large vertebrates from the shape of the vertebral column. *Paleontology* **39**, 80–812.
- Domning DP** (2001) The earliest known fully quadrupedal sirenian. *Nature* **413**, 625–627.
- Domning DP** (2002) The terrestrial posture of desmostylians. *Smith Cont Paleobiol* **93**, 99–111.
- Domning DP, Barnes LG** (2007) A new name for the ‘Stanford skeleton’ of *Paleoparadoxia* (Mammalia, Desmostylia). *J Vertebr Paleont* **27**, 748–751.
- Flynn JJ, Finarelli JA, Zehr S, et al.** (2005) Molecular phylogeny of the Carnivora (Mammalia): Assessing the impact of increased sampling on resolving enigmatic relationships. *Syst Biol* **54**, 317–337.
- Fujiwara SI** (2009) Olecranon orientation as an indicator of elbow joint angle in the stance phase and estimation of forelimb posture in extinct quadruped animals. *J Morph* **270**, 1107–1121.
- Fujiwara SI, Kuwazuru O, Inuzuka N, et al.** (2009) Relationship between scapula position and structural strength of rib cage in quadruped animals. *J Morph* **270**, 1084–1094.
- Fujiwara SI, Hutchinson JR** (2012) Elbow joint adductor moment arm as an indicator of forelimb posture in extinct quadrupedal tetrapods. *Proc Roy Soc Lond B: Biol Sci* **279**, 2561–2570.
- Gingerich PD** (2003) Land-to-sea transition in early whales: Evolution of Eocene Archaeoceti (Cetacea) in relation to skeletal proportions and locomotion of living semiaquatic mammals. *Paleobiology* **29**, 429–454.
- Gray NM, Kimberly K, Madar S, et al.** (2007) Sink or swim? Bone buoyancy control in early cetaceans. *Anat Rec* **290**, 638–653.
- Hayashi S, Houssaye A, Nakajima Y, et al.** (2013) Bone inner structure suggests increasing aquatic adaptations in Desmostylia (Mammalia, Afrotheria). *PLoS ONE* **8(4)**, e59146. doi: 10.1371/journal.pone.0059146.
- Houssaye A** (2009) “Pachyostosis” in aquatic amniotes: a review. *Integr Zool* **4**, 325–340.
- Howell AB** (1930) *Aquatic Mammals; Their Adaptations to Life in the Water*. Springfield, IL: Charles C. Thomas Publisher.
- Inuzuka N** (1984) Skeletal restoration of the desmostylians: herpetiform mammals. *Mem Fac Sci, Kyoto Univ, Ser Biol* **9**, 157–253.
- Inuzuka N** (1996) Body size and mass estimates of desmostylians (Mammalia). *J Geol Soc Japan*, **102**, 816–819.
- Inuzuka N** (2005) The Stanford skeleton of *Paleoparadoxia* (Mammalia: Desmostylia). *Bull Ashoro Mus Paleont* **3**, 3–110.
- Inuzuka N** (2009) The skeleton of *Desmostylus* from Utanobori, Hokkaido, Japan, 2. Postcranial skeleton. *Bull Geol Surv Japan* **60**, 257–379.
- Keaveny TM, Morgan EF, Yeh OC** (2003) Bone mechanics. In *Standard Handbook of Biomedical Engineering and Design* (ed Kutz M), pp. 8.1–8.23. New York: McGraw-Hill.

- Khoshelham K, Elberink SO** (2012) Accuracy and resolution of Kinect depth data for indoor mapping applications. *Sensors* **12**, 1437–1454.
- Lipps JH, Mitchell E** (1976) Trophic model for the adaptive radiations and extinctions of pelagic marine mammals. *Paleobiology* **2**, 147–155.
- Madar SI, Thewissen JGM, Hussain ST** (2002) Additional holotype remains of *Ambulocetus natans* (Cetacea, Ambulocetidae), and their implications for locomotion in early whales. *J Vertebr Paleont* **22(2)**, 405–422.
- Nickel R, Schummer A, Seiferle E, et al.** (1986) *The Anatomy of the Domestic Animals. Volume 1: The Locomotor Systems of the Domestic Mammals*. Berlin: Verlag Paul Parey.
- Nishihara H, Satta Y, Nikaido M, et al.** (2005) A retroposon analysis of afrotherian phylogeny. *Mol Biol Evol* **22**, 1823–1833.
- Nowak RM** (1999) *Walker's Mammals of the World (6th edition)*. Baltimore, MD: The Johns Hopkins University Press.
- Pierce SE, Clack JA, Hutchinson JR** (2012) Three-dimensional limb joint mobility in the early tetrapod *Ichthyostega*. *Nature* **486**, 523–526.
- Pyenson ND, Kelley NP, Parham JF** (2014) Marine tetrapod macroevolution: Physical and biological drivers on 250Ma of invasions and evolution in ocean ecosystems. *Palaeogeogr Palaeoclimatol Palaeoecol* **400**, 1–8.
- Shikama T** (1966) Postcranial skeletons of Japanese Desmostylia. *Paleont Soc Japan, Special Paper* **12**, 1–202.
- Stewart DRM** (1963) The Arabian oryx (*Oryx leucoryx* Pallas). *Afr J Ecol* **1**, 103–117.
- Suto I, Kawamura K, Hagimoto S, et al.** (2012) Changes in upwelling mechanisms drove the evolution of marine organisms. *Palaeogeogr Palaeoclimatol Palaeoecol* **339**, 39–51.
- Thewissen JGM, Hussain ST, Arif M** (1994) Fossil evidence for the origin of aquatic locomotion in archaeocete whales. *Science* **263**, 210–212.
- Thewissen JGM, Williams EM, Roe LJ, et al.** (2001) Skeletons of terrestrial cetaceans and the relationship of whales to artiodactyls. *Nature* **413**, 277–281.
- Thewissen JGM, Cooper LN, George JC, et al.** (2009) From land to water: the origin of whales, dolphins, and porpoises. *Evo Edu Outreach* **2**, 272–288.
- Tokunaga S** (1939) A new fossil mammal belonging to the Desmostylidae. In *Jubilee Publication Commemorating Prof. H. Yabe, M.I.A., Sixtieth Birthday* **1**, pp. 289–299. Sendai: Institute of Geology and Paleontology, Tohoku Imperial University.
- Vogel S** (2003) *Comparative Biomechanics: Life's Physical World*. Princeton, NJ: Princeton University Press.
- Wang Q, Yang C** (2013) The phylogeny of the Cetartiodactyla based on complete mitochondrial genomes.

Int J Biol **5**, published online. doi: 10.5539/ijb.v5n3p31.

Witmer LM (1995) The extant phylogenetic bracket and the importance of reconstructing soft tissues in fossils. In *Functional Morphology in Vertebrate Paleontology*. (ed Thomason JJ), pp. 19–33. New York:Cambridge University Press.

Yamazaki N, Ikeuchi M (2000) Restoration of *Desmostylus* walking by quadrupedal musculo-skeletal robot. *Bull Ashoro Mus Paleont* **1**, 159–165.

Table 1. List of specimens used in this study. Identification number (IN); classification; species; specimen number; life styles (LS: A, obligate aquatics; S, semi-aquatics; T, terrestrial; X, unknown); body mass (BM [kg]); thoracic strength (TF [N]: sum of the fracture loads in the true ribs); the ratio of TF to the total rib strengths (RF [N]: sum of fracture loads in all ribs) (TF/RF [N/N]); and literature referenced for the ecology and body mass data are listed. ID for each specimen is linked to all figures or tables.

IN	Classification	Species	Specimen	LS	BM (kg)	TF (N)	TF/RF	Reference
CETARTIODACTYLA								
Tylopoda								
01	Camelidae	<i>Lama glama</i>	KPM-NF 1004950	T	92.5	9,550	0.94	Nowak, 1999
Ruminantia								
02	Tragulidae	<i>Tragulus javanicus</i>	NSMT M 42386	T	4.35	474	0.97	from the specimen
03	Giraffidae	<i>Giraffa camelopardalis</i>	KPM-NF 1001994	T	550	49,300	0.94	Nowak, 1999
04	Bovidae	<i>Bos gaurus</i>	KPM-NF 1004453	T	825	77,400	0.92	Nowak, 1999
05		<i>Bubalus depressicornis</i>	KPM-NF 1001986	T	225	19,200	0.93	Nowak, 1999
06		<i>Tragelaphus eurycerus</i>	KPM-NF 1002669	T	185	19,400	0.90	Nowak, 1999
07		<i>Oreamnos americanus</i>	KPM-NF 1004520	T	93.0	10,500	0.91	Nowak, 1999
08		<i>Oryx leucoryx</i>	KPM-NF 1004595	T	54.5	3,930	0.82	Stewart, 1963
Whippomorpha								
09	Hippopotamidae	<i>Choeropsis liberiensis</i>	NSMT M 31204	S	215	27,700	0.86	Nowak, 1999
10		<i>Hippopotamus amphibius</i>	NSMT M 948	S	1,000	78,200	0.78	Nowak, 1999
Cetacea								
11	Ambulocetidae	<i>Ambulocetus natans</i> †	NSM PV 20703	X	300	11,600	0.37	Thewissen et al., 1994
12	Balaenopteryidae	<i>Balaenoptera brydei</i>	NSMT M 34505	A	11,500	35,600	0.18	from the specimen
13	Delphinidae	<i>Grampus griseus</i>	KPM-NF 1004648	A	425	6,590	0.67	Nowak, 1999
14		<i>Lagenorhynchus obliquidens</i>	KPM-NF 1004643	A	124	5,500	0.87	Nowak, 1999
15		<i>Orcinus orca</i>	PNPA-Ma 1.2.4.	A	1,590	58,600	0.85	from the specimen
16	Monodontidae	<i>Delphinapterus leucas</i>	NSMT M 34189	A	1,500	54,200	0.77	Nowak, 1999
17	Kogiidae	<i>Kogia sima</i>	KPM-NF 1005210	A	136	6,560	0.73	Nowak, 1999
18	Ziphiidae	<i>Berardius bairdii</i>	NUM unnumbered	A	11,400	260,000	0.87	Nowak, 1999
CARNIVORA								
19	Ursidae	<i>Ursus maritimus</i>	NSMT M 31421	S	350	72,200	0.93	from the specimen
20	Mustelidae	<i>Lutrogale perspicillata</i>	NSMT M 4590	S	9.00	2,980	0.93	Nowak, 1999
21		<i>Enhydra lutris</i>	NSMT M 37707	S	23.5	6,720	0.93	Nowak, 1999
22	Phocidae	<i>Phoca largha</i>	KPM-NF 1001967	S	81.0	14,400	0.87	from the specimen
22	Felidae	<i>Felis catus</i>	SIF 005	T	2.60	1,490	0.95	from the specimen
PAENUNGULATA								
Hyracoidea								
24	Procaviidae	<i>Procavia capensis</i>	NSMT M 34889	T	3.62	563	0.76	from the specimen
Proboscidea								
25	Elephantidae	<i>Elephas maximus</i>	KPM-NF 1004114	T	2,720	263,000	0.78	Nowak, 1999
Sirenia;								
26	Dugongidae	<i>Dugong dugon</i>	NSMT M 26449	A	295	33,400	0.61	Nowak, 1999
27	Trichechidae	<i>Trichechus senegalensis</i>	KPM-NF 1003745	A	500	8,250	0.40	Nowak, 1999
Desmostylia								
28	Desmostylidae	<i>Desmostylus hesperus</i> †	GPM Fo-1	X	1,470	106,000	0.68	Inuzuka, 2005
29	Paleoparadoxiidae	<i>Paleoparadoxia tabatai</i> †	GPM Fo-47	X	993	23,100	0.72	Inuzuka, 1996
30		<i>Neoparadoxia repenningi</i> †	GPM Fo-49	X	2,510	68,100	0.74	Inuzuka, 2005

Life styles of extant taxa were based on Howell (1930).

Abbreviations: GPM, Gifu Prefectural Museum, Seki, Japan; KPM, Kanagawa Prefectural Museum, Odawara, Japan; NSM, National Museum of Nature and Science, Tokyo, Japan; NSMT, Tsukuba Research Departments, National Museum of Nature and Science, Tsukuba, Japan; NUM, Nagoya University Museum, Nagoya, Japan; PNPA, Port of Nagoya Public Aquarium, Nagoya, Japan; SIF, personal collection of Shin-ichi Fujiwara, NUM. Dagger marks indicate extinct species.

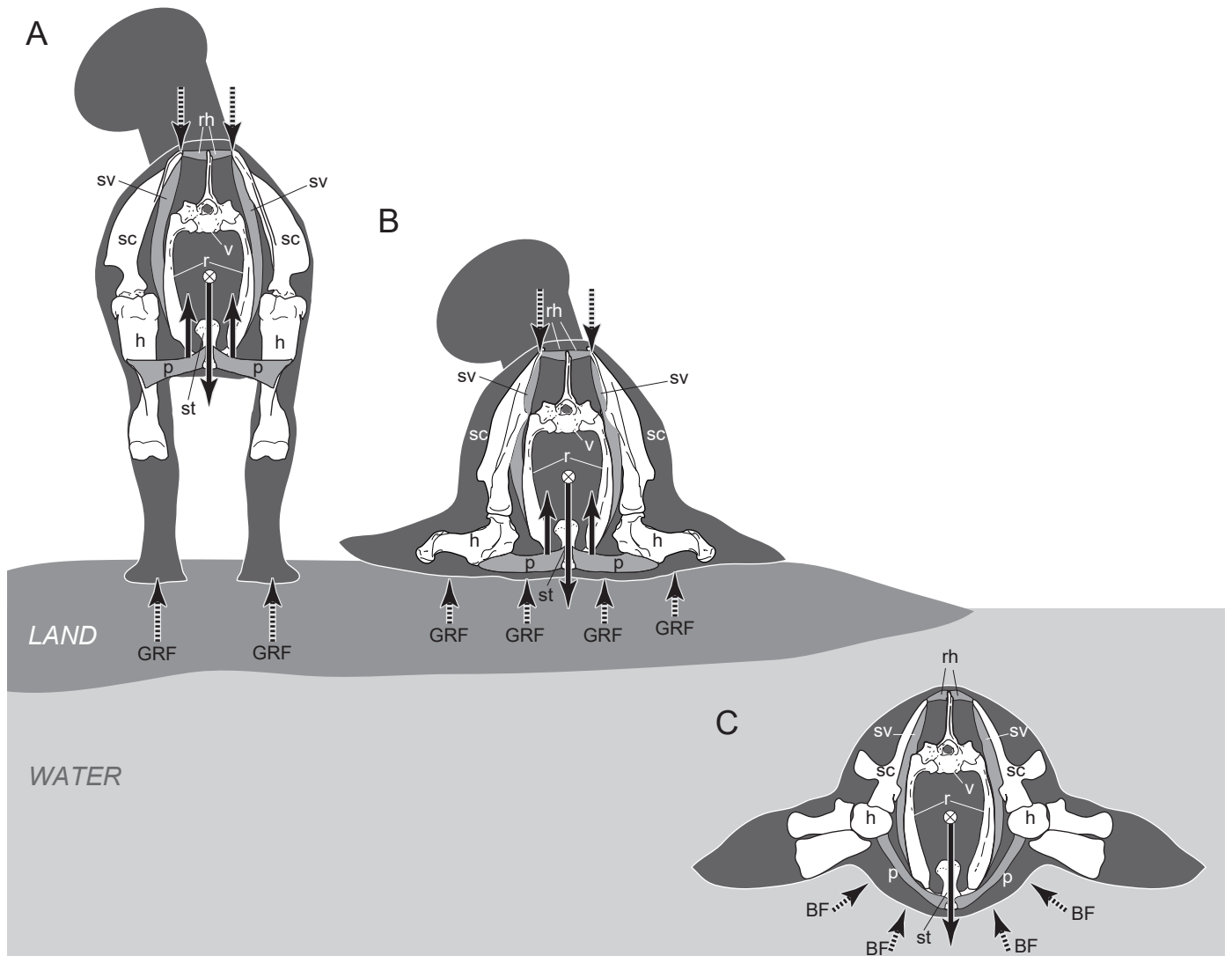
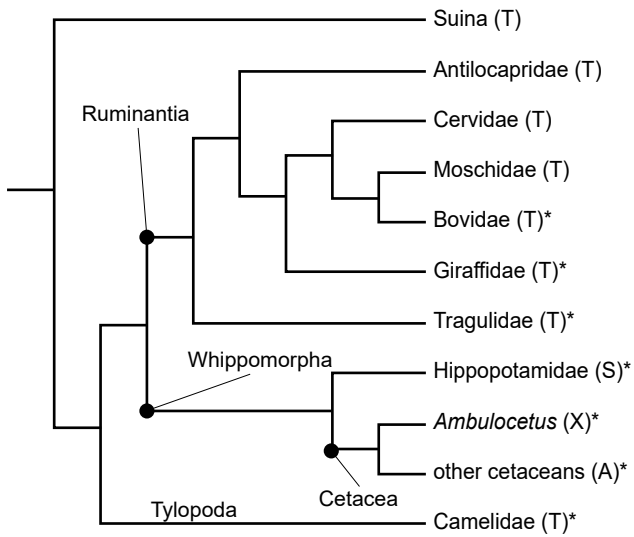
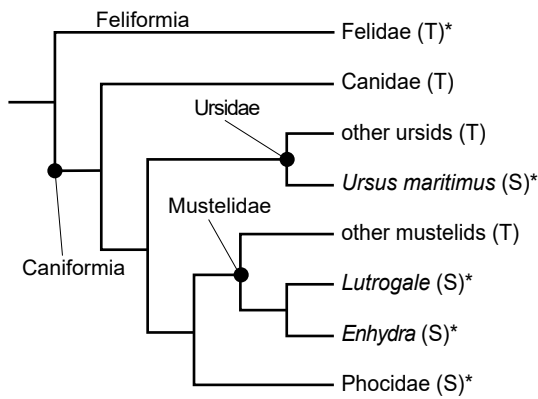


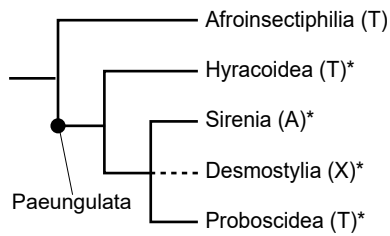
Fig. 1. Mechanical models of thoracic ribs of mammals in terrestrial stances (A) on forelimbs and (B) on thorax; and (C) in the water. The body weights of animals (the downward solid arrows) is balanced by the upward ground reaction force (GRF) or by upward components of the buoyancy forces (BF). In (A) and (B), the thoracic ribs are subjected to compressive force between the body weight and GRF, which is transmitted to the distal end of the ribs via forelimb skeleton/sternum and the thoracic muscles, such as *m. serratus ventralis* and *m. pectoralis*. Abbreviations: h, humerus; p, *m. pectoralis*; r, rib; rh, *m. rhomboideus*; sc, scapula; sv, *m. serratus ventralis*; st, sternum; v, vertebra.



A) Cetartiodactyla



B) Carnivora



C) Afrotheria

Fig. 2. Phylogenetic relationships in (A) Cetartiodactyla (Wang and Yang, 2013), (B) Carnivora (Flynn et al., 2005), and (C) Afrotheria (Nishihara et al., 2005). Abbreviations: A, obligate aquatics; S, semi-aquatics; T, terrestrial quadrupeds; X, unknown. Asterisks: The taxa which include the study taxa.

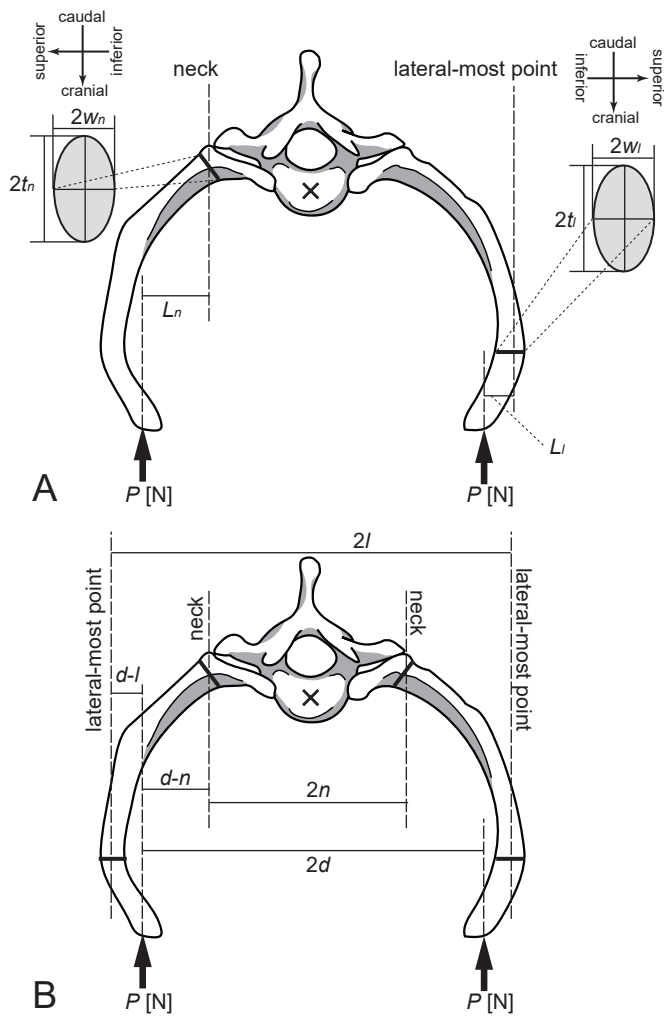


Fig. 3. A) Mechanical models of an arch formed by a vertebra and associated ribs in dorsal-side-up position. The centrum (cross) is fixed to avoid translations and rotations, and the distal end of each rib is subjected to a vertical load (P [N]). The arch is vertically compressed between the upward lifting force ($2P$ [N] in total) and the downward reaction force ($-2P$ [N]) on the centrum. B) Measurements taken from mounted skeletons. The width ($2w$) and the thickness ($2t$) of the transverse section of the rib, and the distances between the necks ($2n$), the lateral-most points ($2l$), and the distal ends ($2d$) on the left and right ribs are shown. The moment arms L_n and L_l were calculated as equations “ $|d - n|$ ” and “ $|d - l|$ ”, respectively.

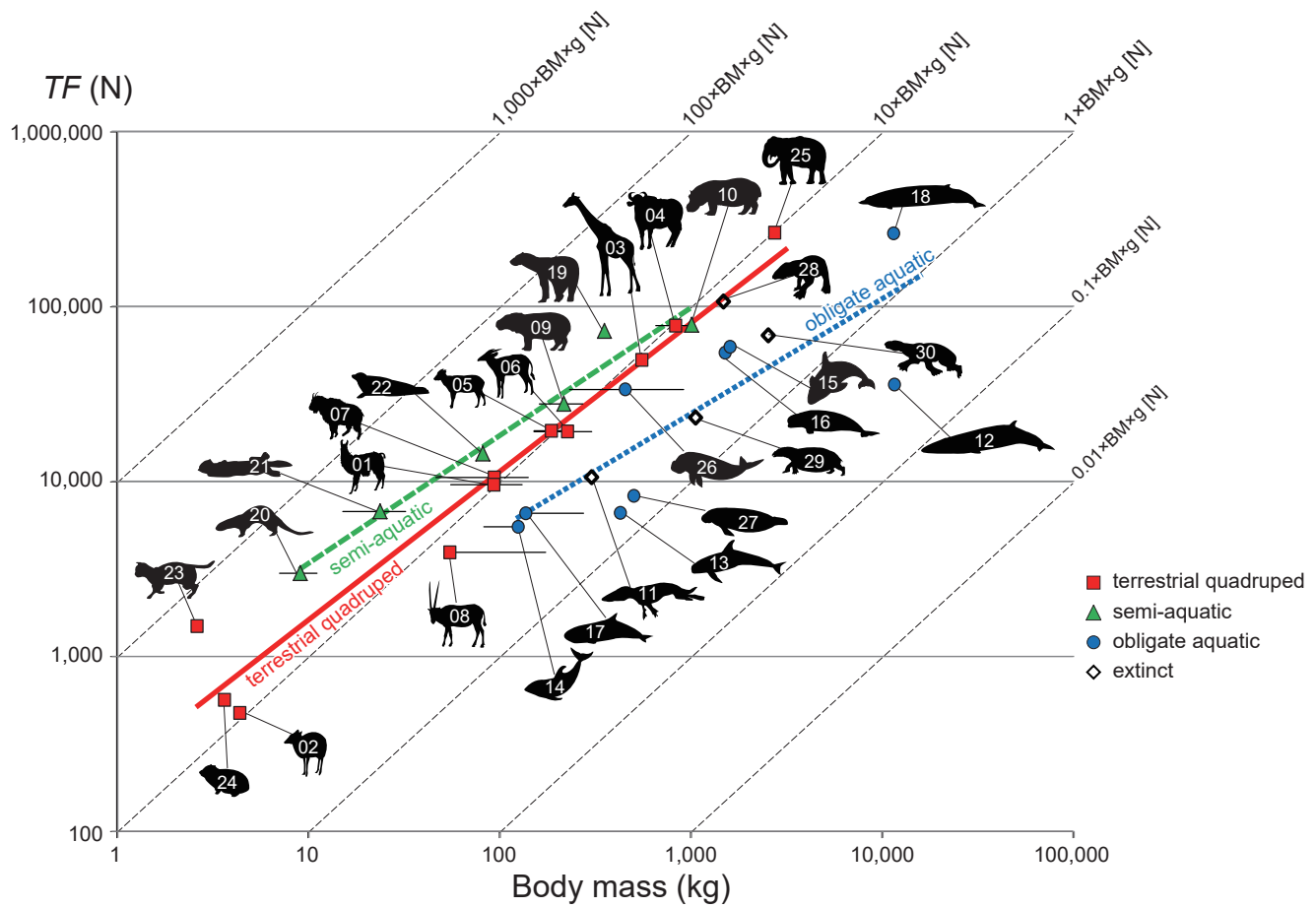


Fig. 4. Relationship between the body mass (BM [kg]) and the thoracic strengths (TF [N]) in study specimens on double logarithmic plots. Equations of the regression lines are as follows: $TF=228.44 \times BM^{0.8489}$ in terrestrial quadrupeds; $TF=632.48 \times BM^{0.7306}$ in semi-aquatics; and $TF=259.36 \times BM^{0.6577}$ in obligate-aquatics. The oblique coordinate system between the dashed lines and the vertical line indicates the relationship between the body mass (kg) and the safety factors (N/N) of the thoraxes, which is defined as the thoracic strengths (TF) standardized by the body weight ($BM \times g$, where g is a standard gravitational acceleration [9.8065 m/s²]). Horizontal bar for each plot indicates the range from minimum to maximum body mass (Nowak, 1999). See Table 1 (for the identification numbers (IN) of the study specimens).

Table S1. Fracture loads of ribs. Rib number (x : x th rib); rib used for measurements (side: R, right rib; L, left rib); type of rib (type: T, true rib; F, false rib; Fl, floating rib; N, rib which has no articulation to the vertebra); and width ($2w$), thickness ($2t$), and medio-lateral distance from the distal end of the rib to the measured point (L), fracture load on the pair of ribs ($2F$), and $2F$ standardized by the body weight ($2^*F/BW$), are shown for the neck (n) and the lateral curves (l) on the rib. F_n and F_l which is lower is indicated in asterisk. See Table 1 for the body mass.

IN	Genus	x	side	type	neck (n)					lateral curve (l)				
					$2t_n$ (mm)	$2w_n$ (mm)	L_n (mm)	$2F_n$ (N)	$2^*F_n/BW$	$2t_l$ (mm)	$2w_l$ (mm)	L_l (mm)	2^*F_l (N)	$2^*F_l/BW$
01	<i>Lama</i> (KPM-NF 1004950)	1	R	T	7.30	12.8	11.5	3440 *	3.80	—	—	—	—	—
		2	R	T	7.65	13.6	36.0	1310 *	1.45	—	—	—	—	—
		3	R	T	6.85	15.9	29.0	1980 *	2.18	19.0	4.90	7.00	2180	2.40
		4	R	T	6.00	16.7	11.0	5080	5.60	21.9	5.30	25.0	821 *	0.905
		5	R	T	9.05	15.5	40.0	1810	2.00	26.0	6.10	26.5	1220 *	1.34
		6	R	T	10.1	10.0	69.0	484 *	0.533	29.0	6.20	23.0	1620	1.78
		7	R	T	10.4	8.85	92.0	294 *	0.324	27.4	5.65	19.0	1540	1.69
		8	R	F	9.05	7.75	93.0	195 *	0.215	24.6	5.30	21.0	1100	1.21
		9	R	F	10.5	5.75	96.0	121 *	0.133	19.1	4.75	18.5	776	0.86
		10	R	F	10.9	5.20	106	92.8 *	0.102	18.2	4.55	21.0	599	0.660
		11	L	F	9.75	5.80	145	75.5 *	0.0832	16.7	3.80	5.50	1460	1.61
		12	R	F	10.2	5.35	103	94.6 *	0.104	14.0	3.70	10.0	640	0.705
02	<i>Tragulus</i> NSMT M 42386	1	R	T	1.44	3.75	1.90	356	8.34	1.63	2.71	4.30	92.9 *	2.18
		2	R	T	1.78	3.08	0.200	2820	66.1	0.950	4.16	4.00	137 *	3.22
		3	R	T	1.60	3.29	4.00	145	3.39	1.02	4.08	4.40	129 *	3.02
		4	R	T	1.35	2.96	8.50	46.4 *	1.09	1.37	4.21	4.60	176	4.13
		5	R	T	1.46	2.89	9.00	45.2 *	1.06	1.22	3.96	6.00	106	2.49
		6	R	T	1.56	2.10	15.3	15.0 *	0.352	1.31	3.67	4.50	131	3.07
		7	R	T	1.45	1.73	17.4	8.33 *	0.195	1.58	2.67	2.60	145	3.39
		8	R	F	1.43	1.48	28.0	3.73 *	0.0875	3.35	1.13	1.20	119	2.79
		9	R	X	1.47	1.32	33.6	2.54 *	0.0596	2.71	1.00	0.10	905	21.2
		10	R	X	1.45	1.17	37.5	1.77 *	0.0414	—	—	—	—	—
		11	R	X	1.55	1.22	32.4	2.38 *	0.0557	—	—	—	—	—
		12	R	X	1.76	1.57	31.6	4.58 *	0.107	—	—	—	—	—
		13	R	X	1.97	1.00	33.3	1.97 *	0.0463	—	—	—	—	—
03	<i>Giraffa</i> KPM-NF 1001994	1	R	T	16.5	29.2	44.6	10500 *	1.95	—	—	—	—	—
		2	R	T	16.4	25.3	8.45	41300	7.66	24.4	11.9	20.4	5590 *	1.04
		3	R	T	14.6	26.1	16.8	19700	3.65	32.6	12.2	13.3	12100 *	2.24
		4	R	T	14.7	28.2	34.1	11400	2.11	33.6	12.8	24.3	7510 *	1.39
		5	R	T	16.6	32.0	62.2	9070	1.68	34.4	14.4	40.0	5940 *	1.10
		6	R	T	15.3	31.8	79.4	6480	1.20	35.9	15.1	61.4	4410 *	0.818
		7	R	T	14.2	28.5	85.8	4460	0.827	33.4	11.8	79.9	1930 *	0.357
		8	R	T	14.4	26.3	95.6	3480	0.645	27.3	11.6	91.7	1340 *	0.248
		9	R	F	13.2	13.5	123	650 *	0.121	22.1	10.3	92.0	851	0.158
		10	R	F	14.6	11.3	131	469 *	0.0870	13.7	19.9	87.0	2080	0.386

Table S1. (cont.)

IN	Genus	x	side	type	neck (n)					lateral curve (l)				
					2t _n (mm)	2w _n (mm)	L _n (mm)	2F _n (N)	2*F _n /BW	2t _l (mm)	2w _l (mm)	L _l (mm)	2*F _l (N)	2*F _l /BW
03	<i>Giraffa</i>	11	R	F	18.5	10.8	141.0	511 *	0.0947	13.9	14.5	75.0	1290	0.239
		12	R	F	18.3	11.1	157.0	476 *	0.0882	15.8	13.2	63.5	1440	0.267
		13	R	F	18.1	10.8	168.0	416 *	0.0770	15.6	12.1	53.6	1420	0.264
		14	R	F	18.2	10.8	170.0	415 *	0.0769	15.4	14.2	34.7	2970	0.551
04	<i>Bos</i> KPM-NF 1004453	1	R	T	15.4	20.7	4.50	48700 *	6.02	11.5	27.8	2.00	148000	18.3
		2	L	T	11.8	19.4	1.00	148000	18.3	7.40	23.8	14.5	9610 *	1.19
		3	L	T	12.6	25.4	13.0	20800	2.57	9.25	27.5	47.0	4970 *	0.614
		4	L	T	11.9	24.9	28.0	8800	1.09	28.4	10.4	38.0	2670 *	0.330
		5	L	T	13.5	24.0	48.5	5350	0.661	35.2	11.4	36.5	4140 *	0.512
		6	L	T	15.7	25.7	52.0	6610	0.817	34.1	13.3	52.0	3840 *	0.475
		7	L	F	16.1	25.8	103	3470 *	0.429	39.6	13.8	41.5	6010	0.743
		8	L	F	15.3	25.2	139	2320 *	0.287	44.4	14.9	47.0	7000	0.865
		9	L	F	14.2	24.2	130	2120 *	0.262	40.5	13.2	63.0	3740	0.462
		10	L	F	15.1	17.3	193	775 *	0.0957	38.9	10.8	36.0	4210	0.520
		11	L	F	14.8	16.8	190	734 *	0.0907	31.9	9.65	37.0	2680	0.331
		12	L	F	17.5	13.6	218	494 *	0.0611	27.7	8.55	18.0	3760	0.464
		13	L	Fl	17.0	14.9	199	631 *	0.0780	23.6	13.3	16.0	8640	1.07
		14	L	Fl	12.3	5.95	203	71.6 *	0.00885	—	—	—	—	—
05	<i>Bubalus</i> KPM-NF 1001986	1	R	T	6.80	17.2	21.9	3070 *	1.39	—	—	—	—	—
		2	R	T	7.00	17.0	11.1	6110	2.77	15.9	6.20	10.2	1990 *	0.904
		3	R	T	7.65	16.6	3.75	18800	8.50	20.3	6.75	9.65	3200 *	1.45
		4	R	T	8.75	16.3	24.5	3170 *	1.44	22.8	7.85	7.95	5900	2.67
		5	R	T	10.2	16.9	39.1	2460 *	1.11	24.7	6.50	13.0	2680	1.21
		6	R	T	12.9	17.8	49.6	2740 *	1.24	24.5	8.50	21.5	2750	1.25
		7	R	T	12.4	17.6	70.5	1810	0.820	26.3	5.70	19.8	1440 *	0.653
		8	R	T	12.7	14.9	80.8	1160 *	0.526	28.5	7.35	25.4	2020	0.915
		9	R	F	12.3	11.5	109	492 *	0.223	26.3	5.85	12.6	2390	1.08
		10	R	F	15.1	10.5	122	455 *	0.206	24.6	8.50	6.90	8580	3.89
		11	R	F	13.5	9.55	142	289 *	0.131	—	—	—	—	—
		12	R	F	10.2	7.90	148	143 *	0.0648	—	—	—	—	—
		13	R	F	11.5	6.35	135	114 *	0.0518	—	—	—	—	—
06	<i>Tragelaphus</i> KPM-NF 1002669	1	R	T	9.50	18.6	8.50	12900	7.11	9.80	17.6	11.0	9210 *	5.08
		2	R	T	8.80	16.6	11.5	7040	3.88	6.05	14.8	17.5	2530 *	1.39
		3	R	T	8.00	18.9	6.50	14600	8.05	17.2	7.60	24.0	1380 *	0.759
		4	R	T	8.85	19.2	19.0	5730	3.16	20.7	7.80	27.0	1550 *	0.856
		5	R	T	9.45	18.4	22.5	4750	2.62	22.1	7.30	42.0	934 *	0.515
		6	R	T	10.3	19.0	75.0	1650 *	0.907	21.4	9.55	26.0	2500	1.38
		7	R	T	12.4	18.6	53.0	2680	1.48	22.8	10.6	39.0	2170 *	1.20
		8	R	F	10.6	12.7	73.5	770 *	0.425	26.3	9.35	39.5	1940	1.07

Table S1. (cont.)

IN	Genus	x	side	type	neck (n)					lateral curve (l)				
					2t _n (mm)	2w _n (mm)	L _n (mm)	2F _n (N)	2*F _n /BW	2t _l (mm)	2w _l (mm)	L _l (mm)	2*F _l (N)	2*F _l /BW
06	<i>Tragelaphus</i>	9	R	F	9.25	10.5	85.5	394 *	0.217	21.9	8.45	37.5	1390	0.767
		10	R	X	9.70	9.35	92.5	306 *	0.169	22.0	7.95	39.0	1190	0.654
		11	R	X	12.0	10.0	165	242 *	0.133	18.4	8.55	9.00	4980	2.74
		12	R	X	8.80	10.0	151	195 *	0.107	14.1	6.45	7.50	2610	1.44
		13	R	X	13.2	8.40	108	288 *	0.159	—	—	—	—	—
07	<i>Oreamnos</i> KPM-NF 1004520	1	R	T	12.1	9.47	10.5	3440 *	3.77	15.7	9.85	11.5	4420	4.85
		2	R	T	7.10	13.7	12.5	3560	3.90	14.1	6.70	14.5	1450 *	1.59
		3	R	T	8.65	13.7	4.00	13400	14.7	14.6	5.75	10.1	1600 *	1.75
		4	R	T	8.76	12.3	35.5	1240 *	1.36	15.3	5.85	6.00	2900	3.18
		5	R	T	10.7	13.0	20.0	3000	3.29	15.8	6.35	21.0	1010 *	1.11
		6	R	T	11.3	13.1	20.0	3210	3.52	17.4	6.95	33.5	837 *	0.92
		7	R	T	10.9	12.2	58.0	926	1.02	17.8	6.10	24.0	921 *	1.01
		8	R	F	9.10	9.35	78.0	340 *	0.373	15.4	10.7	12.0	4890	5.36
		9	R	F	8.10	8.40	88.5	216 *	0.236	13.1	6.35	16.0	1100	1.21
		10	R	F	7.25	7.85	123	121 *	0.133	9.50	6.15	2.00	6000	6.58
		11	R	F	6.90	7.60	118	113 *	0.124	—	—	—	—	—
		12	R	F	9.30	7.20	112	144 *	0.158	—	—	—	—	—
		13	R	F	8.55	6.60	137	90.7 *	0.100	—	—	—	—	—
08	<i>Oryx</i> KPM-NF 1004595	1	R	T	10.5	5.98	17.5	718 *	1.34	11.5	6.81	18.0	991	1.85
		2	R	T	9.16	5.44	8.00	1130	2.12	10.6	4.80	12.5	649 *	1.21
		3	R	T	10.2	5.65	8.00	1360	2.54	12.8	4.83	12.0	831 *	1.56
		4	R	T	10.8	6.29	3.50	4060	7.60	13.5	4.98	21.5	521 *	0.98
		5	R	T	11.2	6.48	39.0	403 *	0.753	14.2	4.86	21.0	532	1.00
		6	R	T	11.6	7.56	57.5	385 *	0.721	14.9	5.17	12.5	1060	1.98
		7	R	T	10.5	8.31	57.5	420 *	0.786	15.9	5.24	22.5	648	1.21
		8	R	F	10.9	8.03	92.5	253 *	0.474	14.2	5.48	12.5	1140	2.13
		9	R	X	10.3	7.11	95.0	182 *	0.341	13.9	5.02	20.0	585	1.09
		10	R	X	10.4	6.85	103	158 *	0.296	12.7	5.09	18.5	593	1.11
		11	R	X	9.81	6.80	135	112 *	0.210	9.23	4.75	6.00	1160	2.17
		12	R	X	8.24	7.25	142	102 *	0.190	—	—	—	—	—
		13	R	X	8.44	5.62	123	72.6 *	0.136	—	—	—	—	—
09	<i>Choeropsis</i> NSMT M 31240	1	R	T	10.4	12.6	18.3	3010 *	1.43	—	—	—	—	—
		2	R	T	11.7	15.2	5.45	16500 *	7.84	21.6	12.8	1.45	82000	38.9
		3	R	T	13.2	19.0	19.2	8290	3.93	23.4	9.09	29.1	2220 *	1.05
		4	R	T	12.6	16.8	45.5	2620	1.24	21.9	9.91	29.5	2430 *	1.15
		5	R	T	13.2	16.1	61.7	1850 *	0.876	9.58	23.5	15.0	11800	5.60
		6	R	T	15.0	15.4	72.4	1640 *	0.777	10.5	21.9	21.0	7980	3.79
		7	R	F	15.1	15.0	74.7	1520 *	0.719	13.9	15.9	33.9	3450	1.64
		8	R	F	15.8	11.9	95.3	775 *	0.368	13.5	14.4	30.1	3120	1.48

Table S1. (cont.)

IN	Genus	x	side	type	neck (n)					lateral curve (l)				
					2t _n (mm)	2w _n (mm)	L _n (mm)	2F _n (N)	2*F _n /BW	2t _l (mm)	2w _l (mm)	L _l (mm)	2*F _l (N)	2*F _l /BW
09	<i>Choeropsis</i>	9	R	F	17.1	11.3	109	676 *	0.321	13.1	11.9	28.5	2190	1.04
		10	R	F	16.9	11.3	119	604 *	0.287	12.3	11.9	27.4	2130	1.01
		11	R	F	16.2	8.92	147	293 *	0.139	14.0	10.2	17.9	2710	1.28
		12	R	F	16.9	8.20	160	236 *	0.112	13.2	11.4	6.60	8620	4.09
		13	R	F	15.7	8.15	166	210 *	0.100	15.4	8.18	5.90	5810	2.76
		14	R	Fl	15.9	8.17	168	212 *	0.101	18.7	8.28	1.65	25900	12.3
		15	R	Fl	15.2	6.68	145	156 *	0.0740	13.1	7.65	3.50	7320	3.47
10	<i>Hippopotamus</i> NSMT M 948	1	R	T	15.8	22.7	32.2	8430 *	0.860	—	—	—	—	—
		2	R	T	15.8	25.0	20.8	15800	1.61	32.9	14.3	22.0	10200 *	1.04
		3	R	T	19.5	34.7	15.0	52300	5.33	36.6	19.2	25.3	17800 *	1.81
		4	R	T	20.9	36.5	38.9	23900 *	2.44	35.2	18.2	16.2	24100	2.45
		5	R	T	20.7	35.1	74.5	11400 *	1.16	32.5	13.8	18.0	11500	1.17
		6	R	T	21.0	31.3	106	6450 *	0.658	28.2	17.3	16.4	17100	1.74
		7	R	F	22.2	31.7	121	6150 *	0.627	23.8	15.3	20.2	9180	0.937
		8	R	F	27.2	26.3	151	4160 *	0.424	23.0	17.8	18.0	13500	1.37
		9	R	F	29.1	25.4	177	3540 *	0.361	19.1	17.9	7.60	26800	2.73
		10	R	F	29.1	22.2	197	2430 *	0.248	24.7	13.8	1.10	143000	14.6
		11	R	F	32.2	20.1	202	2150 *	0.220	20.9	14.4	0.550	262000	26.7
		12	R	F	25.7	20.7	215	1700 *	0.174	—	—	—	—	—
		13	R	Fl	25.0	13.6	214	718 *	0.0732	—	—	—	—	—
		14	R	Fl	21.2	19.1	209	1240 *	0.126	—	—	—	—	—
		15	R	Fl	18.0	11.5	192	414 *	0.0422	—	—	—	—	—
11	<i>Ambulocetus</i> NSM PV 20703	1	L	T	17.2	21.9	116	2380 *	0.807	—	—	—	—	—
		2	L	T	14.7	21.3	131	1700 *	0.576	—	—	—	—	—
		3	L	T	16.6	22.1	130	2090 *	0.711	23.9	21.5	11.3	32700	11.1
		4	L	T	17.3	21.8	149	1860 *	0.631	20.8	25.6	7.35	61900	21.0
		5	L	T	21.3	22.1	137	2530 *	0.862	17.0	21.8	9.05	29900	10.1
		6	L	F	17.1	21.1	131	1930 *	0.657	29.2	15.9	4.80	51600	17.5
		7	L	F	17.9	18.8	132	1600 *	0.544	27.6	16.1	3.85	62000	21.1
		8	L	F	20.4	11.2	123	694 *	0.236	17.9	19.4	8.20	27400	9.30
		9	L	F	19.0	17.4	122	1570 *	0.534	17.0	19.0	12.5	16400	5.57
		10	L	F	19.7	18.1	115	1880 *	0.640	18.7	17.2	15.2	12100	4.13
		11	L	F	19.1	18.3	114	1880 *	0.639	18.8	18.1	17.1	12000	4.09
		12	L	F	17.6	17.7	106	1740 *	0.590	18.2	19.8	27.1	8810	2.99
		13	L	Fl	19.6	14.7	93.5	1500 *	0.510	19.8	19.6	36.0	7040	2.39
		14	L	Fl	23.6	14.2	108	1470 *	0.499	18.5	22.4	18.6	16700	5.68
		15	L	Fl	22.8	20.4	87.5	3620 *	1.23	21.8	17.4	6.50	33900	11.5
12	<i>Balaenoptera</i> NSMT M 34505	1	L	T	19.6	65.4	236	11900 *	0.105	37.5	90.8	381	27100	0.240
		2	L	F	33.0	86.8	165	50300	0.446	35.2	82.2	334	23800 *	0.211

Table S1. (cont.)

IN	Genus	x	side	type	neck (n)					lateral curve (l)				
					$2t_n$ (mm)	$2w_n$ (mm)	L_n (mm)	$2F_n$ (N)	$2*F_n/BW$	$2t_l$ (mm)	$2w_l$ (mm)	L_l (mm)	$2*F_l$ (N)	$2*F_l/BW$
15	<i>Orcinus</i> PNPA-Ma 1.2.4.	1	L	T	19.6	58.3	69.2	16100 *	2.06	22.5	47.2	33.0	25400	3.25
		2	L	T	20.2	54.9	158	6460 *	0.828	62.9	21.2	28.5	16600	2.13
		3	L	T	20.6	45.1	196	3580 *	0.459	45.1	20.8	43.5	7480	0.959
		4	L	T	24.1	44.0	245	3170 *	0.406	41.4	20.7	39.5	7500	0.962
		5	L	F	25.9	45.5	261	3430 *	0.440	40.8	19.3	52.0	4900	0.628
		6	L	F	30.5	41.6	273	3220 *	0.413	41.7	20.0	62.0	4490	0.576
		7	L	F	38.3	33.9	328	2240 *	0.287	39.9	19.6	29.5	8660	1.11
		8	L	F	34.1	30.5	319	1650 *	0.212	37.9	17.8	24.0	8340	1.07
		9	L	FL	39.0	24.7	319	1250 *	0.160	36.1	18.6	13.5	15400	1.97
		10	L	Fl	37.6	24.9	292	1330 *	0.171	29.0	15.9	10.5	11600	1.49
		11	L	Fl	36.6	20.9	243	1100 *	0.141	29.0	11.8	1.50	45200	5.79
16	<i>Delphinapterus</i> NSMT M 34189	1	R	T	23.2	54.0	85.0	26600 *	1.81	20.0	39.7	2.50	422000	28.7
		2	R	T	16.5	44.3	124	8700 *	0.591	34.4	16.9	0.50	652000	44.4
		3	R	T	14.5	40.4	123	6450 *	0.438	36.3	16.5	34.5	9540	0.649
		4	R	T	14.7	35.6	129	4810 *	0.327	31.1	19.9	63.5	6470	0.440
		5	R	T	14.8	30.1	177	2530 *	0.172	29.7	16.5	37.0	7280	0.495
		6	R	T	23.2	32.3	158	5120 *	0.348	30.2	18.0	52.0	6290	0.427
		7	R	F	22.0	26.2	142	3570	0.242	26.2	16.2	74.0	3100 *	0.211
		8	R	X	25.9	26.3	112	5360	0.364	27.0	15.8	82.0	2740 *	0.186
		9	R	X	25.7	23.6	147	3250	0.221	25.2	11.7	37.0	3100 *	0.211
		10	R	X	26.6	31.2	116	7480	0.508	28.5	10.8	30.0	3710 *	0.252
		11	R	X	38.8	17.5	123	3240 *	0.220	29.1	9.60	23.5	3810	0.259
17	<i>Kogia</i> KPM-NF 1005210	1	R	T	6.25	20.4	36.5	2380 *	1.78	8.40	24.4	15.0	11100	8.31
		2	R	T	5.95	21.1	21.0	4190	3.14	25.9	7.65	65.0	778 *	0.584
		3	L	F	5.95	19.5	49.0	1540	1.16	20.8	8.00	56.0	792 *	0.594
		4	R	X	7.95	19.0	94.5	1010 *	0.760	18.7	9.05	40.0	1280	0.958
		5	R	X	7.55	18.1	90.5	907 *	0.680	16.7	9.00	49.5	909	0.682
		6	R	X	9.75	16.9	134	694 *	0.520	15.8	8.85	26.0	1580	1.19
		7	R	X	12.3	15.6	155	638 *	0.478	16.1	8.90	13.5	3150	2.36
		8	R	X	11.4	10.7	150	289 *	0.217	17.4	8.30	9.00	4430	3.32
		9	R	X	15.8	10.0	142	373 *	0.279	—	—	—	—	—
		10	R	X	18.4	9.20	133	392 *	0.294	—	—	—	—	—
		11	R	X	17.6	8.70	80.0	556 *	0.417	—	—	—	—	—
		12	R	X	12.7	7.65	122	203 *	0.152	—	—	—	—	—
18	<i>Berardius</i> NUM unnumbered	1	R	T	25.5	112	159	67600 *	0.606	42.3	85.4	22.2	464000	4.16
		2	R	T	23.9	95.9	65.4	112000 *	1.00	37.9	83.6	75.4	117000	1.05
		3	R	T	33.5	76.3	224	29100 *	0.261	28.9	73.4	69.2	75100	0.673
		4	R	T	30.8	82.4	243	28700 *	0.257	29.9	58.4	114	29800	0.267
		5	R	T	32.9	62.9	443	9800 *	0.088	73.9	29.0	31.3	66100	0.592

Table S1. (cont.)

IN	Genus	x	side	type	neck (n)					lateral curve (l)				
					2t _n (mm)	2w _n (mm)	L _n (mm)	2F _n (N)	2*F _n /BW	2t _l (mm)	2w _l (mm)	L _l (mm)	2*F _l (N)	2*F _l /BW
18	<i>Berardius</i> NUM unnumbered	6	R	T	40.8	60.1	265	18600	0.166	62.9	26.7	114	13100 *	0.117
		7	R	F	32.9	66.0	225	21300	0.191	63.6	27.5	117	13700 *	0.122
		8	R	X	36.0	50.4	292	10500 *	0.0938	67.7	26.1	48.6	31800	0.285
		9	R	X	52.0	50.4	640	6880 *	0.0617	—	—	—	—	—
		10	R	X	58.4	39.2	457	6550 *	0.0587	—	—	—	—	—
19	<i>Ursus</i> NSMT M 31421	1	R	T	16.3	35.5	8.50	80200	23.4	11.4	28.7	6.20	50800 *	14.8
		2	R	T	12.5	28.8	34.0	10100 *	2.95	6.75	21.0	3.90	25400	7.39
		3	R	T	10.8	25.9	89.5	2700 *	0.787	—	—	—	—	—
		4	R	T	10.0	24.3	99.5	1980 *	0.578	10.2	20.2	1.35	102000	29.8
		5	R	T	10.7	24.6	118	1830 *	0.533	17.3	8.63	12.6	3430	1.00
		6	R	T	11.0	24.2	125	1720 *	0.502	15.9	10.6	14.1	4250	1.24
		7	R	T	11.4	25.4	132	1850 *	0.539	14.4	11.6	11.5	5610	1.63
		8	R	T	10.6	22.7	157	1160 *	0.339	13.1	9.59	3.40	11800	3.44
		9	R	F	11.3	23.6	167	1260 *	0.367	—	—	—	—	—
		10	R	X	11.8	21.0	184	951 *	0.277	—	—	—	—	—
		11	R	X	12.8	20.1	178	972 *	0.283	—	—	—	—	—
		12	R	X	11.6	18.5	172	768 *	0.224	—	—	—	—	—
		13	R	X	12.1	17.0	150	778 *	0.227	—	—	—	—	—
		14	R	X	14.8	13.5	175	516 *	0.150	—	—	—	—	—
20	<i>Lutrogale</i> NSMT M 4590	1	R	T	3.30	6.80	1.13	4510	51.1	4.11	3.46	1.49	1100 *	12.5
		2	R	T	3.57	6.20	8.75	524 *	5.93	—	—	—	—	—
		3	R	T	3.11	6.58	14.3	315 *	3.57	3.81	3.63	0.05	33500	380
		4	R	T	3.14	6.17	19.2	208 *	2.36	3.19	3.13	0.51	2070	23.4
		5	R	T	2.97	5.59	21.7	143 *	1.62	2.72	3.31	1.48	672	7.62
		6	R	T	3.01	5.24	23.0	120 *	1.36	2.89	3.58	2.50	496	5.61
		7	R	T	3.11	5.09	23.2	116 *	1.32	2.81	4.05	4.35	354	4.01
		8	R	T	3.14	5.04	20.3	131 *	1.49	2.97	4.12	5.38	313	3.54
		9	R	T	3.65	4.59	21.1	122 *	1.38	2.77	4.11	4.86	321	3.64
		10	R	T	3.51	5.10	22.3	137 *	1.55	2.65	3.95	3.90	354	4.01
		11	R	T	3.33	3.84	25.1	65.4 *	0.740	3.12	4.09	2.36	737	8.35
		12	R	F	4.10	3.31	25.1	59.8 *	0.678	3.40	3.84	2.39	702	7.95
		13	R	F	4.54	3.90	20.4	113 *	1.28	3.20	3.59	6.58	209	2.37
		14	R	Fl	3.34	3.60	23.4	61.8 *	0.700	4.18	2.72	0.67	1550	17.6
21	<i>Enhydra</i> NSMT M 37707	1	L	T	4.89	12.2	5.65	4320	18.8	4.26	8.47	2.97	3430 *	14.9
		2	L	T	5.80	8.97	25.8	605 *	2.62	4.31	7.08	1.22	5910	25.6
		3	L	T	6.32	8.57	34.2	453 *	1.97	5.79	4.92	2.40	1950	8.48
		4	R	T	6.07	9.37	66.5	268 *	1.16	5.86	5.94	1.50	4600	20.0
		5	L	T	7.12	8.72	60.4	299 *	1.30	6.94	5.70	7.33	1030	4.45
		6	L	T	7.00	8.59	54.2	318 *	1.38	9.90	6.54	9.92	1430	6.19

Table S1. (cont.)

IN	Genus	<i>x</i>	side	type	neck (<i>n</i>)					lateral curve (<i>l</i>)				
					$2t_n$ (mm)	$2w_n$ (mm)	L_n (mm)	$2F_n$ (N)	$2^*F_n/BW$	$2t_l$ (mm)	$2w_l$ (mm)	L_l (mm)	2^*F_l (N)	$2^*F_l/BW$
21	<i>Enhydra</i> NSMT M 37707	7	L	T	7.43	8.49	71.3	251 *	1.09	9.75	6.63	5.54	2580	11.2
		8	L	T	8.18	7.94	80.2	215 *	0.931	12.0	7.72	6.40	3740	16.2
		9	L	T	8.50	8.51	90.1	228 *	0.990	12.7	7.07	1.10	19200	83.5
		10	L	T	8.54	9.02	89.1	260 *	1.13	10.7	7.55	5.00	4080	17.7
		11	L	T	9.38	11.7	109	390 *	1.69	10.0	7.38	2.60	6980	30.3
		12	L	F	8.73	9.47	129	202 *	0.877	—	—	—	—	—
		13	L	X	9.68	8.14	126	170 *	0.738	—	—	—	—	—
		14	L	X	8.57	7.90	114	156 *	0.677	—	—	—	—	—
22	<i>Phoca</i> KPM-NF 1001967	1	R	T	7.95	17.9	18.7	4530 *	5.71	—	—	—	—	—
		2	R	T	7.55	18.0	28.0	2920 *	3.67	—	—	—	—	—
		3	R	T	6.75	14.7	38.0	1280 *	1.61	—	—	—	—	—
		4	R	T	6.95	15.2	44.5	1210 *	1.52	—	—	—	—	—
		5	R	T	9.75	13.1	46.6	1200 *	1.51	—	—	—	—	—
		6	R	T	8.60	13.5	66.9	782 *	0.984	—	—	—	—	—
		7	R	T	8.30	14.3	75.4	752 *	0.947	—	—	—	—	—
		8	R	T	8.80	13.7	84.1	651 *	0.819	—	—	—	—	—
		9	R	T	8.55	13.5	92.3	564 *	0.710	—	—	—	—	—
		10	R	T	8.45	13.5	100	514 *	0.647	—	—	—	—	—
		11	R	F	8.55	13.0	111	433 *	0.546	—	—	—	—	—
		12	R	F	7.70	13.4	115	400 *	0.503	—	—	—	—	—
		13	R	F	7.20	14.8	116	452 *	0.569	—	—	—	—	—
		14	R	Fl	8.05	11.7	108	341 *	0.429	—	—	—	—	—
		15	R	Fl	9.45	13.4	94.0	598 *	0.753	—	—	—	—	—
23	<i>Felis</i> SIF 005	1	R	T	1.94	3.73	0.43	2120	83.1	2.88	2.46	0.90	650 *	25.5
		2	L	T	1.84	3.93	2.80	339 *	13.3	2.98	1.80	0.13	2580	101
		3	L	T	1.85	3.78	4.67	189 *	7.42	3.17	2.06	1.25	361	14.1
		4	L	T	2.43	3.68	9.85	112 *	4.37	3.08	1.92	1.07	356	14.0
		5	L	T	2.18	3.86	15.2	71.6 *	2.81	—	—	—	—	—
		6	L	T	1.96	3.56	19.2	43.2 *	1.69	—	—	—	—	—
		7	L	T	2.29	3.74	21.0	51.0 *	2.00	—	—	—	—	—
		8	L	T	1.99	3.39	24.6	31.1 *	1.22	—	—	—	—	—
		9	L	F	2.22	2.96	28.1	23.1 *	0.906	—	—	—	—	—
		10	L	F	2.27	3.05	33.4	21.1 *	0.828	—	—	—	—	—
		11	L	F	2.21	2.64	33.4	15.4 *	0.604	—	—	—	—	—
		12	L	Fl	2.00	2.08	39.5	7.32 *	0.287	—	—	—	—	—
		13	L	Fl	1.83	1.75	38.2	4.90 *	0.192	—	—	—	—	—
24	<i>Procapra</i> NSMT M 34889	1	L	T	2.38	4.98	6.50	303	8.54	2.40	3.43	6.50	145 *	4.08
		2	L	T	1.54	4.40	3.50	284	8.01	1.76	2.90	4.50	110 *	3.09
		3	L	T	1.50	4.38	11.0	87.3 *	2.46	1.91	2.34	1.80	194	5.46

Table S1. (cont.)

IN	Genus	x	side	type	neck (n)					lateral curve (l)						
					2t _n (mm)	2w _n (mm)	L _n (mm)	2F _n (N)	2*F _n /BW	2t _l (mm)	2w _l (mm)	L _l (mm)	2*F _l (N)	2*F _l /BW		
24	<i>Procapia</i> NSMT M 34889	4	L	T	1.42	4.65	13.5	75.9 *	2.14	2.07	2.45	2.50	166	4.67		
		5	L	T	1.60	4.69	20.5	57.3 *	1.61	—	—	—	—	—		
		6	L	T	1.93	4.78	28.5	51.6 *	1.45	—	—	—	—	—		
		7	L	T	1.68	4.68	34.0	36.1 *	1.02	—	—	—	—	—		
		8	L	F	1.77	4.30	41.0	26.6 *	0.751	—	—	—	—	—		
		9	L	F	1.80	3.33	42.0	15.9 *	0.447	—	—	—	—	—		
		10	L	F	1.83	3.96	31.5	30.4 *	0.857	—	—	—	—	—		
		11	L	F	1.58	3.82	38.7	19.9 *	0.560	—	—	—	—	—		
		12	L	X	1.65	3.30	40.0	15.0 *	0.422	—	—	—	—	—		
		13	L	X	1.85	3.63	40.0	20.3 *	0.573	—	—	—	—	—		
		14	R	X	1.68	3.14	35.5	15.6 *	0.439	—	—	—	—	—		
		15	L	X	1.63	2.19	43.5	6.00 *	0.169	—	—	—	—	—		
		16	L	X	1.68	2.70	43.0	9.51 *	0.268	—	—	—	—	—		
		17	L	X	2.21	1.62	40.5	4.78 *	0.135	—	—	—	—	—		
		18	L	X	2.44	1.48	39.5	4.52 *	0.127	—	—	—	—	—		
		19	L	X	2.37	1.72	40.5	5.78 *	0.163	—	—	—	—	—		
		20	L	X	2.04	1.42	38.0	3.61 *	0.102	—	—	—	—	—		
		21	L	X	1.88	1.33	32.5	3.42 *	0.0962	—	—	—	—	—		
		25	<i>Elephas</i> KPM-NF 1004114	1	L	T	63.6	42.5	57.1	67300 *	2.52	—	—	—	—	—
				2	L	T	34.7	70.4	22.4	256000	9.61	30.9	77.0	80.1	76300 *	2.86
				3	L	T	33.7	63.5	81.3	55800 *	2.09	60.8	30.8	30.5	63000	2.36
4	L			T	29.1	66.7	124	34700 *	1.30	58.7	36.2	29.7	86400	3.24		
5	L			T	51.3	35.8	223	9860 *	0.370	52.7	33.1	26.5	72900	2.73		
6	L			T	31.4	45.2	235	9110 *	0.342	53.7	28.2	37.9	37500	1.40		
7	L			F	31.1	48.1	241	9960 *	0.373	48.7	23.2	10.5	82800	3.10		
8	L			F	37.7	47.0	401	6940 *	0.260	—	—	—	—	—		
9	L			F	30.5	46.6	448	4950 *	0.185	—	—	—	—	—		
10	L			F	37.6	42.7	399	5720 *	0.215	—	—	—	—	—		
11	L			F	41.1	40.5	367	6130 *	0.230	—	—	—	—	—		
12	L			F	39.1	38.0	415	4550 *	0.170	—	—	—	—	—		
13	L			F	42.3	34.5	461	3640 *	0.137	—	—	—	—	—		
14	L			F	36.6	39.0	387	4790 *	0.180	—	—	—	—	—		
15	L			F	44.8	41.3	395	6460 *	0.242	—	—	—	—	—		
16	L			F	40.5	35.2	406	4120 *	0.154	—	—	—	—	—		
17	L			F	41.4	34.9	424	3970 *	0.149	—	—	—	—	—		
18	L			F	44.9	34.0	379	4580 *	0.172	—	—	—	—	—		
19	L			F	36.0	25.1	299	2530 *	0.0950	—	—	—	—	—		
20	L			F	46.7	33.3	113	15300 *	0.572	—	—	—	—	—		

Table S1. (cont.)

IN	Genus	x	side	type	neck (n)					lateral curve (l)				
					$2t_n$ (mm)	$2w_n$ (mm)	L_n (mm)	$2F_n$ (N)	$2*F_n/BW$	$2t_l$ (mm)	$2w_l$ (mm)	L_l (mm)	$2*F_l$ (N)	$2*F_l/BW$
26	<i>Dugong</i> NSMT M 26449	1	L	T	11.1	38.7	53.0	10500 *	2.37	—	—	—	—	—
		2	L	T	15.6	38.1	94.0	8040 *	1.82	19.0	33.1	26.3	26400	5.99
		3	L	T	17.1	36.7	121	6340 *	1.44	19.4	30.6	7.50	80800	18.3
		4	L	T	30.0	33.6	131	8590 *	1.95	22.7	21.5	8.75	39900	9.05
		5	L	F	32.9	26.3	179	4250 *	0.963	—	—	—	—	—
		6	L	X	32.7	22.9	189	3020 *	0.685	—	—	—	—	—
		7	L	X	30.4	20.5	236	1800 *	0.408	—	—	—	—	—
		8	L	X	29.5	19.7	228	1670 *	0.380	—	—	—	—	—
		9	L	X	27.3	18.0	240	1230 *	0.279	—	—	—	—	—
		10	L	X	26.9	17.2	262	1010 *	0.229	—	—	—	—	—
		11	L	X	25.6	16.6	254	930 *	0.211	—	—	—	—	—
		12	L	X	26.4	15.0	251	787 *	0.178	—	—	—	—	—
		13	L	X	25.4	16.1	245	897 *	0.203	—	—	—	—	—
		14	L	X	24.0	16.2	249	841 *	0.191	—	—	—	—	—
		15	L	X	22.9	17.2	235	960 *	0.218	—	—	—	—	—
		16	L	X	20.4	16.6	263	716 *	0.162	—	—	—	—	—
		17	L	X	20.8	16.8	228	859 *	0.195	—	—	—	—	—
		18	L	X	16.0	12.9	221	402 *	0.091	—	—	—	—	—
		19	L	X	21.9	21.9	220	1600 *	0.362	—	—	—	—	—
27	<i>Trichechus</i> KPM-NF 1003745	1	R	X	10.2	19.2	61.5	2040 *	0.416	—	—	—	—	—
		2	R	X	11.3	20.6	86.3	1860 *	0.378	13.1	19.2	2.20	73000	14.9
		3	R	X	13.6	21.0	106	1890 *	0.385	12.5	21.0	14.2	13000	2.64
		4	R	X	16.3	25.2	140	2460 *	0.502	13.8	23.2	10.4	23900	4.87
		5	R	X	28.9	19.1	156	2240 *	0.457	13.7	19.9	21.9	8200	1.67
		6	R	X	26.9	19.8	180	1960 *	0.399	15.2	21.8	21.6	11200	2.28
		7	R	X	25.0	18.6	214	1340 *	0.273	14.7	20.0	16.1	12200	2.49
		8	R	X	21.9	16.7	219	932 *	0.190	12.5	22.0	18.4	10900	2.23
		9	R	X	21.0	16.9	251	791 *	0.161	14.1	21.8	9.35	23800	4.86
		10	R	X	22.8	17.1	265	837 *	0.171	13.8	19.6	5.70	30900	6.31
		11	R	X	20.5	16.1	275	640 *	0.131	16.5	19.2	4.15	48700	9.93
		12	R	X	21.0	15.0	272	580 *	0.118	17.8	17.3	4.85	36700	7.48
		13	R	X	20.6	17.9	263	837 *	0.171	14.4	18.6	6.55	25300	5.16
		14	R	X	19.9	14.8	247	590 *	0.120	19.5	19.1	10.5	22600	4.60
		15	R	X	19.8	14.5	249	558 *	0.114	24.9	16.5	2.15	104000	21.3
		16	R	X	18.8	12.9	238	439 *	0.0896	—	—	—	—	—
		17	R	X	11.9	18.5	204	663 *	0.135	—	—	—	—	—
28	<i>Desmostylus</i> GPM Fo-1	1	R	T	28.3	36.6	55.7	22800 *	1.58	—	—	—	—	—
		2	R	T	25.4	52.8	95.0	24900 *	1.73	—	—	—	—	—
		3	R	T	20.0	57.6	111	19900 *	1.39	16.0	51.0	6.30	220000	15.3

Table S1. (cont.)

IN	Genus	x	side	type	neck (n)					lateral curve (l)				
					$2t_n$ (mm)	$2w_n$ (mm)	L_n (mm)	$2F_n$ (N)	$2*F_n/BW$	$2t_l$ (mm)	$2w_l$ (mm)	L_l (mm)	$2*F_l$ (N)	$2*F_l/BW$
28	<i>Desmostylus</i> GPM Fo-1	4	L	T	21.6	51.7	155	12500 *	0.867	20.6	48.1	6.05	262000	18.3
		5	L	T	24.7	49.1	160	12400 *	0.865	24.9	45.4	13.8	124000	8.65
		6	L	T	28.3	50.5	174	13900 *	0.965	28.1	40.6	32.4	47700	3.32
		7	L	X	28.8	43.3	162	11100 *	0.773	23.2	35.8	50.0	19900	1.38
		8	R	X	28.9	40.5	160	9880 *	0.687	31.2	37.8	67.1	22100	1.54
		9	R	X	27.5	40.0	137	10700 *	0.748	29.3	41.3	83.5	19900	1.39
		10	L	X	27.6	33.3	173	5880 *	0.409	31.3	22.7	52.9	10100	0.706
		11	L	X	26.7	27.2	168	3920 *	0.273	31.4	21.6	56.6	8640	0.601
		12	L	X	24.4	31.4	152	5290 *	0.368	33.0	20.6	50.4	9320	0.648
		13	L	X	29.5	20.6	161	2600 *	0.181	35.7	20.0	47.5	9980	0.694
29	<i>Paleoparadoxia</i> GPM Fo-47	1	L	X	15.9	39.2	60.4	13500	0.547	24.6	26.5	118	4880 *	0.198
		2	L	X	11.0	34.7	75.3	5870 *	0.238	12.1	32.5	8.06	52900	2.15
		3	L	X	13.9	36.9	144	4390 *	0.178	29.7	19.8	12.9	30100	1.22
		4	L	X	22.0	34.8	245	3620 *	0.147	30.6	29.5	1.49	599000	24.3
		5	L	X	26.2	31.5	321	2710 *	0.110	28.4	27.8	1.69	433000	17.6
		6	L	X	19.8	27.9	313	1650 *	0.0668	—	—	—	—	—
		7	L	X	26.1	23.3	347	1360 *	0.0552	—	—	—	—	—
		8	L	X	26.6	27.6	379	1780 *	0.0723	28.0	15.0	15.8	13200	0.536
		9	L	X	24.9	24.2	393	1240 *	0.0502	—	—	—	—	—
		10	L	X	26.5	24.0	455	1120 *	0.0453	—	—	—	—	—
		11	L	X	19.3	23.9	450	819 *	0.0332	—	—	—	—	—
		12	L	X	23.8	20.3	469	701 *	0.0284	—	—	—	—	—
		13	L	X	20.8	19.0	430	585 *	0.0237	—	—	—	—	—
		14	L	X	21.6	18.3	421	571 *	0.0232	—	—	—	—	—
		15	L	X	21.6	17.1	369	573 *	0.0232	—	—	—	—	—
		16	L	X	16.2	11.4	222	317 *	0.0129	—	—	—	—	—
30	<i>Neoparadoxia</i> GPM Fo-49	1	L	X	18.8	56.5	40.1	50100	1.70	26.9	36.0	88.5	13200 *	0.447
		2	L	X	22.6	53.4	122	17600 *	0.599	—	—	—	—	—
		3	L	X	20.4	54.4	192	10500 *	0.357	—	—	—	—	—
		4	L	X	23.1	62.6	254	11900 *	0.405	53.3	29.1	3.00	503000	17.1
		5	L	X	31.7	49.6	296	8770 *	0.298	—	—	—	—	—
		6	R	X	32.0	44.2	338	6160 *	0.209	42.3	27.2	8.85	118000	4.01
		7	R	X	28.3	39.0	378	3800 *	0.129	41.9	21.1	9.55	65500	2.23
		8	R	X	30.4	38.1	383	3860 *	0.131	41.2	21.2	20.0	30700	1.04
		9	R	X	29.1	34.6	433	2680 *	0.0911	38.3	24.3	5.45	139000	4.72
		10	L	X	34.1	29.4	443	2220 *	0.0755	—	—	—	—	—
		11	L	X	27.3	32.3	457	2080 *	0.0707	—	—	—	—	—
		12	L	X	29.8	30.9	445	2140 *	0.0727	—	—	—	—	—
		13	R	X	39.0	30.3	412	2890 *	0.0984	—	—	—	—	—

Table S1. (cont.)

IN	Genus	x	side	type	neck (n)					lateral curve (l)				
					$2t_n$ (mm)	$2w_n$ (mm)	L_n (mm)	$2F_n$ (N)	$2^*F_n/BW$	$2t_l$ (mm)	$2w_l$ (mm)	L_l (mm)	2^*F_l (N)	$2^*F_l/BW$
30	<i>Neoparadoxia</i>	14	L	X	32.1	24.8	399	1650 *	0.0561	—	—	—	—	—
	GPM Fo-49	15	L	X	39.7	20.8	352	1630 *	0.0555	—	—	—	—	—
		16	L	X	23.0	14.9	232	731 *	0.0248	—	—	—	—	—